reading for static hole error and turbulence in accordance with equation (4.5). This static pressure measurement can then be compared with that determined by means of a pitot-static or static pressure tube at the same point in order to evaluate Δ_p, whence K can be determined.

This method of static pressure measurement should be investigated.

5. SINGLE-PURPOSE STATIC PRESSURE PROBES

Several attempts have been made in the past to develop a probe which will reliably measure static pressure only. A typical design is one in which the pressure is measured at a central hole drilled in the face of a thin circular disc. Experience has shown, however, that such instruments do not operate satisfactorily. The slightest misorientation yields totally unreliable static pressure measurements. When the flow is three-dimensional, in either steady or unsteady flow regimes and at high turbulence levels, the true static pressure is not registered.

The 'needle' static pressure probe suffers similar disadvantages.

The pitot cylinder or the pitot sphere can be used as single-purpose instruments for measuring static pressure. The adverse, and hitherto unpredictable, factors which influence the accuracy of these instruments were dealt with in the foregoing section.

The author therefore attempted to develop a single-purpose static pressure probe based on completely different operating principles.

5.1 The spherical static pressure probe

In the light of the experience gained in the development of the spherical total pressure probe, it was decided to investigate the possibility of determining static pressure from a total pressure measurement together with the corresponding pressure in the wake of a sphere; total pressure can be controlled, by minimising its dependence on Reynolds number and turbulence level, using a trip groove or wire around the circumference of the sphere to stabilise the wake flow characteristics.

5.1.1 Theoretical analysis

Neglecting the effect of turbulence, the total pressure in a free stream flowing at velocity V_o is given by :

$$p_t = p_s + \tfrac{1}{2}\rho V_o^2 \quad \text{.................} \quad (4.16)$$

The pressure in the wake behind a sphere can be written as :

$$P(\text{wake}) = p_s - \frac{K}{2}\rho V_o^{\,2} \quad \ldots\ldots\ldots\ldots\ldots\ldots (4.17)$$

where K* represents a constant to be determined experimentally, its value depending on Reynolds number, turbulence level and Mach number.

Rearranging the above equations yields:

$$\frac{p_s - p(\text{wake})}{\frac{1}{2}\rho V_o^{\,2}} = K, \quad \ldots\ldots\ldots\ldots\ldots\ldots (4.18)$$

and hence by determining the appropriate pressures, K can be calculated at various Reynolds numbers (based on V_o and sphere diameter).

Equations (4.16) and (4.17) also yield :

$$P_t - P(\text{wake}) = \tfrac{1}{2}\rho V_o^{\,2}\,(1 + K)$$

$$\text{or} \quad \frac{P_t - P(\text{wake})}{1 + K} = \frac{\Delta p}{1+K} = \tfrac{1}{2}\rho V_o^{\,2}$$

$$\text{and} \quad p_s = P_t - \tfrac{1}{2}\rho V_o^{\,2}$$

$$\text{Thus,} \quad p_s = P_t - \frac{\Delta p}{1+K} \quad \ldots\ldots\ldots\ldots (4.19)$$

Where Δ_p is the differential pressure relative to the wake pressure.

The experimental objective would therefore be to minimize the effects of Reynolds number and turbulence

* $K \equiv C_p$ the base pressure coefficient for a sphere.

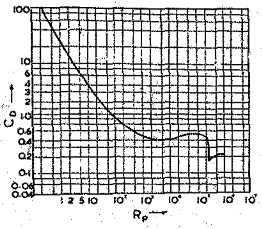

FIG. 4·11 DRAG COEFFICIENT ON SPHERES

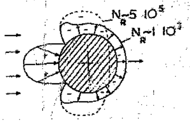

PRESSURE DISTRIBUTION AROUND
A SPHERE

on the value of K, over the range tested, and to establish an average value for K for which a wide range of angular insensitivity in yaw and pitch would be possible.

If this proved feasible, static pressure in a free stream could be determined from equation (4.19), by measuring the total pressure and the pressure differential relative to the wake of the sphere. These pressure measurements could then be corrected as described in this and in the previous chapter.

At the outset, probe sizes and operational velocity range were determined by studying the standard relationship between drag coefficient and Reynolds number for a spherical body (Fig. 4.11). The graph shows that C_D, the drag coefficient, and hence K, would be least dependent on Reynolds number effects over the approximate range $5 \times 10^3 \leq R_p \leq 1 \times 10^5$, where R_p is the probe Reynolds number. It was accordingly decided to select experimental probe diameters ranging from 3/16 inch to ½ inch, whence the speed range of the test rig gave a safe practical Reynolds number range of
$6.75 \times 10^3 \leq R_p \leq 7.2 \times 10^4$.

5.1.2 Test facilities and method of testing

The initial tests were carried out in a

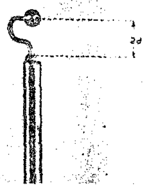

FIG. 4·12 STATIC PRESSURE PROBE No.1 (0·2 INCH DIAMETER SPHERE 0·2 INCH DIAMETER STEM)

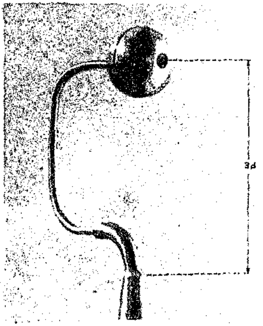

FIG 4·13 STATIC PRESSURE PROBE No.2 (0·5 INCH DIAMETER SPHERE 0·5 INCH DIAMETER STEM) closed 3-inch diameter blower duct assembly as well as on an interchangeable 6-inch free jet for checking purposes.

The second and third test series were conducted in the 7.5-inch diameter closed test section of the diffuser rig at N.E.L. These rigs were used for the development of the cylindrical and spherical total pressure probes.

Suitable wall static tappings were available in the test section and readings were taken at air speeds ranging from approximately 70 to 280 ft/sec. In these tests, the probes on test were used to record the dynamic pressure reference at the centre line of the flow for zero angle of attack.

5.1.2.1 Initial tests

Early tests were conducted to establish a general guide to probe geometry and probe rigidity. The probes tested are shown in Figs. 4.12 and 4.13. The impact orifices were slightly countersunk and both spheres had tripping grooves.

Pressure differentials, relative to wall static pressure, were taken for the probe facing the flow ($\frac{1}{2}\rho v_0^2$), and for the probe turned through 180 degrees

$(p_s - p(\text{wake}))$. The results of 33 measurements with probe No. 1, at different speeds, revealed that K was unstable showing a marked variation with Reynolds number.

The reason for this was thought to lie in the proximity of the sphere to the end of the main stem, and in disturbances caused by the bent supporting tube when the probe was facing downstream.

It was therefore decided to increase the distance between sphere and main stem; to alter the supporting tube configuration, and to increase the sphere diameter to ½ inch in order to ensure better orifice and probe finish and faster response. Accordingly probe No. 2 (Fig. 4.13) was designed and tested in the diffuser rig.

The results confirmed the above diagnosis : The value of K proved to be reasonably stable although still dependent on Reynolds number but to a lesser degree. The main stem and supporting tube bend apparently have a marked influence on instrument performance and should be located at interference-free positions relative to the spherical probe head which, in turn, should be kept as small as practically possible.

5.1.2.2 Test series II

In this series it was decided to adopt a sphere

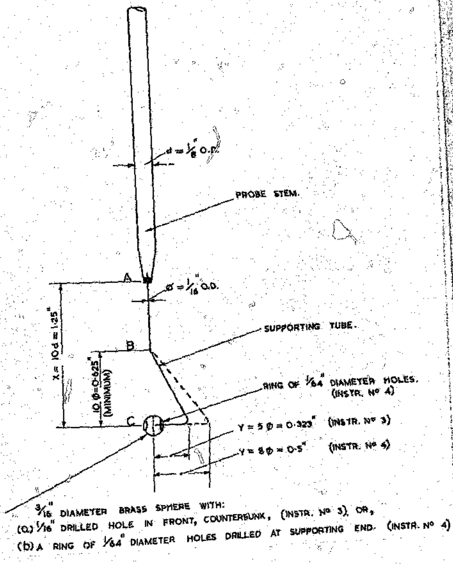

FIG. 4·14 SPHERICAL STATIC PRESSURE PROBES ALTERNATE DESIGNS FOR INSTRS. Nº 3 AND Nº 4 diameter of 3/16 inch, with an 1/8-inch diameter stem. The supporting tube design was altered as shown in Fig. 4.14 to minimize its effect on the wake pressure distribution without loss of rigidity following the increased 'X' dimension ($X = 10_d$). The groove in the sphere was replaced by a trip wire. The resulting instrument, probe No. 3 is shown in Figs. 4.14 and 4.15.

The test results reflected a considerable improvement in the K vs R_p relationship. It was now possible to select an average K-value which did not deviate by more than ± 2 per cent over the entire test range. The yaw and pitch characteristics, however, were most disappointing; the probe with the rounded supporting tube showed poor sensitivity in pitch. The latter result focused attention on the importance of parameter Y.

Due to the greatly increased X-dimension for this probe, it was argued that the probe performance could probably be further improved by eliminating the influence of the supporting tube on the wake pattern. This could be achieved only if the sphere was supported in such a manner that the flow in its wake could take place before reaching the supporting tube.

Thus, the idea originated of supporting the sphere at its wake-end and to tap the pressure behind the sphere

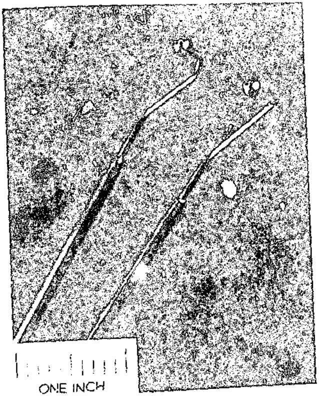

FIG. 4.15 IMPROVED STATIC PRESSURE PROBE

near the support. To accomplish this the original probe orifice was sealed off and minute holes, 1/64-inch diameter, were drilled in the form of a ring round the supporting tube where it enters the spherical head. The dimension Y was increased to 8 $\emptyset$, $\emptyset$ being the brass sphere diameter, in order to increase the range of insensitivity to yaw and pitch and a trip wire was fixed to the sphere. Details of this instrument, probe No. 4, are shown in Fig. 4.14.

5.1.2.3 Test series III

On test, probe No. 4 could not of course be used for determining the reference dynamic pressure ($\frac{1}{2}\rho V_o^2$); a spherical total pressure probe of the type described in Chapter III was introduced from the opposite wall of the duct for measuring this reference pressure.

The results revealed characteristics which were most promising. The value for K was stable at any particular velocity and remained fairly constant, the average value of 0.655 being to within $\pm$ 1 per cent of the measured values over the speed range 70 ft/sec to 280 ft/sec.

The average angular insensitivity over the range was very encouraging, giving approximately $\pm$ 33 degrees in yaw and -15 degrees to +30 degrees in pitch for a K-value to within 1 per cent of dynamic pressure, as

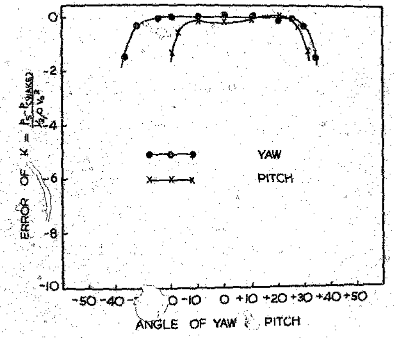

FIG.4·16 VARIATION OF K WITH ANGLE OF ATTACK (INSTR. N° 4) shown in Fig. 4.16. It should be noted that, according to the safe Reynolds number range, this probe should give satisfactory results up to air speeds of approximately 400 ft/sec. At higher speeds, however, the range of angular insensitivity would decrease.

Considering the errors involved, it may be stated that this probe will measure static pressure in oblique flow within an error of less than 2 per cent of the dynamic pressure. Although the instrument is capable of better performance with further development, there are certain restrictions.

Increasing the parameter Y would most probably improve probe performance, especially in pitch positions but, on the other hand, a bigger hole would be needed to accommodate the probe unless distance BC (Fig. 4.14) is increased; this, in turn, could mean forfeiting rigidity. Decreasing dimension AB and increasing BC by increasing Y might, however, be investigated in greater detail in relation to dimension X which dominates the probe stability in pulsating flow.

It is important to note that in evaluating the test results for these probes the corrections for wall static and total pressure readings, in relation to hole size and turbulence, were neglected. The probe characteristics, however, do not appear to be so critical as to be affected appreciably by these corrections.

6. CONCLUSIONS

In concluding this chapter, it may be stated that, depending on the problem, the flow regime, and the accuracies required, static pressure can be measured by means of wall static tappings, combined pitot-static tubes, or single-purpose probes. The author has developed a single-purpose probe which showed reasonable performance characteristics and promise for further development. The wall static tapping method proved to be the most reliable and accurate, provided it was applied with the necessary 'know-how' and corrections.

It has been shown that there are still many complex factors demanding further investigation and clarification whatever the method of measurement adopted. These factors have been identified and analysed and some correction factors have been suggested.

CHAPTER V

THE MEASUREMENT OF VELOCITY OF FLOW BY CURRENT METER

1. INTRODUCTION

In 1790, Woltman (61) invented the screw-type current meter. He developed the theory of these meters and used the instrument for measuring flow velocities in rivers. The meter was improved from time to time and in 1925, L.A. Ott (62) published a new 'Theory of current meters' based on experiments performed over many years at the Mathematical and Mechanical Institute of the firm A. Ott in Germany. The resulting Ott current meter is now considered to be reliable for measuring flow velocities in pipes and channels.

The cup-type current meter was introduced by Farrand Henry in 1867. In 1882, Price developed an improved type which has been widely used ever since, particularly in the U.S.A.

This chapter deals with the screw- or propeller-type current meter with special reference to the small Ott propeller meters which were used by the author in calibration, laboratory and field experiments in the United Kingdon.

2. PROBLEMS ASSOCIATED WITH VELOCITY MEASUREMENT EMPLOYING CURRENT METERS

At a recent symposium on flow measurement in closed conduits, held at N.E.L., (61) attention was drawn to the fact that, although the current meter and pitot tube were among the oldest instruments in use for flow measurement, contributions on the performance and application of these instruments were still topical. When it is appreciated that there are more than 200 papers dealing with pitot tubes and their application and some 300 references to the characteristics and use of current meters, (61) it is remarkable that there remain so many unsolved problems associated with the application of these instruments. With present knowledge in this field, simple solutions to problems are admittedly not possible, but it is submitted that progress has been hampered by the practice of collecting masses of unplanned experimental data, some of it quite irrelevant and unsupported by theoretical analysis and basic thinking.

The calibration and application of current meters are inseparable functions. A current meter should be applied under conditions similar to those at which it was calibrated, or a meter should be calibrated according to the dictates of actual experimental conditions. This is seldom, if ever, realised in practice.

As shown in Chapter I, considerable research has been done on the effects of the various factors affecting the performance of current meters, but there still remain many unknowns. Theories about these uncertainties have been advanced by many experts who differ markedly among themselves. The following are some examples of controversial factors : A meter is rated by towing through still water, away from solid boundaries, after which it is applied in turbulent or oblique flows near flume and pipe walls. The effects of meter supporting frames, waiting periods in between rating runs, proximity and velocity gradients are, among others, still sources of speculation when conditions of rating and application differ.

It is encouraging to learn that experts are now planning to pool the research efforts and facilities of various countries in order to evaluate these effects accurately.[61]

Here, the author attempts to analyse the basic principles affecting the operation of propeller-type current meters with the object of clarifying and defining the problems that demand further investigation and solution.

The factors may be listed thus :

The practice of rating by towing through still water;

The effect of the supporting current meter frame;

The effect of meter positions relative to solid boundaries and to adjacent meters;

The effect of temperature and pressure;

The effect of waiting periods in rating tests;

The effect of submergence;

Oblique flow effects;

The effect of turbulence;

The effect of steep velocity gradients;

The effect of inertia;

The effect of Reynolds number;

The effect of meter position and number in a cross-section;

Recording, servicing, and care.

The aim is to analyse the physical mechanisms rather than to study only experimental findings.

3. THEORY AND ANALYSIS

3.1 The fundamental current meter equation

When an ideal helical propeller is driven at a speed of 'n' revolutions per unit time by a perfect fluid flowing at average local velocity 'v', the relationship between velocity and speed of revolution has the following simple form :

$$V = K_a n \quad \ldots\ldots\ldots\ldots\ldots\ldots\ldots\ldots\ldots\ldots\ldots\ldots \quad (5.1)$$

where K_a denotes the geometrical pitch of the propeller. Complex mechanical and hydraulic resistance forces, however, modify the above expression.

At present, no rigorous mathematical analysis has been advanced to correlate theory with experimental results. An approximate solution, suggested by L.A. Ott, [62] yields a semi-empirical relationship embodying constants which have to be determined by experiment. It is submitted that theoretical development and a thorough understanding of the characteristic equation of a current meter must precede a factor analysis.

The author, using dimensional analysis, has determined the form of the basic equation. Following Ott's general suggestions, [62] the following fundamental factors are analysed :

3.1.1 The torque developed by the blades;

3.1.2 The moment due to external hydraulic resistance forces;

3.1.3 The moment due to internal mechanical resistance forces.

3.1.1 <u>Torque</u>

The torque, T_b, developed by the passage of fluid through the blades, can be expressed thus ;

$$T_b = \rho V^2 K_a{}^3 \phi' \left(\frac{S}{K_a}, \frac{\upsilon}{VK_a}, \frac{K_a n}{V}\right) \qquad (5.2)$$

where V = average local velocity;

ρ = mass density of fluid;

K_a = geometrical pitch of propeller;

S = a theoretical length dimension associated with blade shape as defined;

υ = kinematic viscosity;

n = number of revolutions per unit time;

ϕ' = notation denoting 'function'.

Equation (5.2) emerged from dimensional analysis aided by Buckingham's Π-theorem.

When employing equation (5.2) to determine the torque exerted by a flow medium on a particular meter, the dimensionless parameter $\frac{S}{K_a}$ and the factor $\rho K_a{}^3$ can be embodied in an instrument constant to be determined experimentally. This coefficient will depend on the particular blade shape, the hydraulic pitch, and the fluid density.

Under normal conditions and flow velocities of up to say 9 ft/sec, the flow in the blade boundary layers would probably be laminar. Calibration curves indeed show that the effect of Reynolds number over the particu-

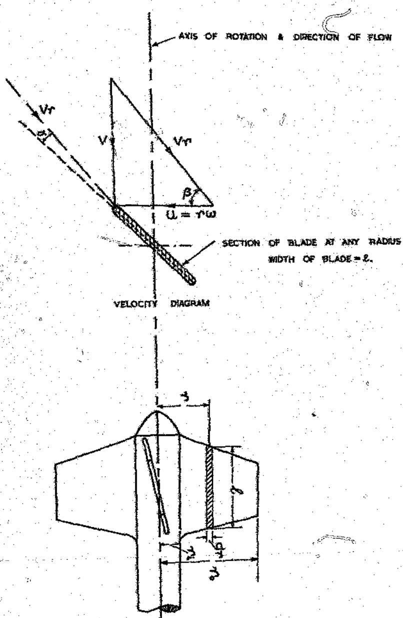

FIG. 5-1 PROPELLER METER SHOWING VELOCITY DIAGRAM FOR BLADE SECTION AT A PARTICULAR RADIUS (DIAGRAMATIC)

lar speed range is negligible. The author submits that at high velocities when the boundary-layer flow is purely turbulent the same argument would apply and the Reynolds number effect would again be masked by other influences. In the transition zone, however, it seems logical to argue that the Reynolds number effect would become important. The break sometimes displayed in a calibration curve seems to corroborate this. Thus, outside the transition range of flow velocities the term $\frac{\upsilon}{VK_a}$, can be neglected as an influence on torque.

Equation (5.2) can therefore be written as :

$$T_b \;=\; C_o\, V^2\, \phi^n\, \left(\frac{K_a n}{V}\right) \;\ldots\ldots\ldots\ldots\ldots\ldots\ldots\ldots\ldots\ldots\ldots \;(5.3)$$

where C_o represents the instrument coefficient defined above.

In an attempt to evaluate the functional relationship expressed by equation (5.3), the following analysis was made :

The vector diagram for flow past the blade of a propeller-type current meter is shown in Fig. 5.1.

If σF is the force, due to flow, on an elementary blade section at radius r, the torque developed can be written as :

$$\sigma T \;=\; \sigma F.\sigma A.r \;\ldots\ldots\ldots\ldots\ldots\ldots\ldots\ldots\ldots\ldots\ldots\ldots\ldots \;(5.4)$$

Now σF can be expressed as :

$\sigma F \;=\; C_L \tfrac{1}{2}\rho V^2 \mathrm{Sin}\beta$, where C_L is the coefficient of lift on the blade section and dependent on the angle of attack α.

Also, σA represents the elementary area on the chord at radius r or,

$$\sigma A \;=\; \ell dr$$

Hence equation (5.4) can be written as :

$$\sigma T \;=\; \tfrac{1}{2} C_L \rho V_r^2 \ell dr \mathrm{Sin}\,\beta . r$$

from which it follows that :

$$T \;=\; \int \sigma T \;=\; \int_{r_i}^{r_o} C_L \rho\,(V^2 + U^2)\,\ell\, \mathrm{Sin}\;\beta . r . dr \;\ldots\ldots (5.5)$$

On examining the above equation, one can write :

$$C_L \;=\; f(\alpha)$$

and hence $\quad C_L \;=\; F'(r)\;;\;\; \ell = f''(r)$ and

$$\mathrm{Sin}\,\beta \;=\; f'''(r)$$

Therefore equation (5.5) can be written as :

$$T \;=\; C_o' \int_{r_i}^{r_o} F(r)\,(V^2 + U^2)\;.\,dr \;\ldots\ldots\ldots (5.6)$$

or $\quad T \;=\; C_o'\,\left(\int_{r_i}^{r_o} V^2 . F(r) . dr + \int_{r_i}^{r_o} U^2 . F(r) . dr\right)$

Now at a particular free stream velocity V,

$\int_{r_i}^{r_o} V^2.F(r).dr$ can be expressed as :

K_1V^2 in evaluated form;

also $\int_{r_i}^{r_o} U^2.F(r).dr = \int_{ri}^{ro} r^2\omega^2 F(r).dr,$

where ω = angular speed of rotation, and the above equation can be written in evaluated form, as :

$$\int_{r_i}^{r_o} r^2\omega^2.F(r).dr = K_2\theta(K_an)^2 \quad \text{where } K_an = V.$$

Thus equation (5.6) can be written as :

$$T = C_o' \quad (K_1V^2 + K_2\,\theta\,(K_an)^2\,)$$

or $$T = C_o'' \; (\,V^2 + \theta'(K_an)^2\,) \quad \ldots\ldots\ldots\ldots\ldots\ldots(5.7)$$

On comparing equations (5.3) and (5.7) a solution is suggested, because the hydrodynamic force on the blades is equal to the rate of change of axial momentum of the fluid passing through the meter. Due to the forces of friction, the theoretical velocity, as registered by the meter, i.e. K_an at n revolutions per unit time, is less than V, the actual flow velocity. This discrepancy is due to the energy absorbed in overcoming mechanical and hydraulic forces of resistance and hence to the change in momentum yielding a force per unit mass rate of flow which is proportional to $(V-K_an)$.

Thus, equation (5.7) suggests that the above relationship can be written as :

$$T = C''_o (V^2 - (K_a n)^2) \quad \text{.....................} (5.8)$$

and equation (5.3) suggests that the expression could be of the form :

$$T_b = C_o V^2 (1 - \frac{K_a n}{V}) \quad \text{.....................} (5.9)$$

It is therefore clear that if, in equation (5.8), $(K_a n)^2$ is written as $K_a n \cdot V$, $(K_a n \approx V)$ equation (5.8) is identical to equation (5.9). Therefore the basic equation for torque can be defined as :

$$T_b = C_o V^2 (1 - \frac{K_a n}{V}) \quad \text{.....................} (5.10)$$

where C_o is a constant to be determined experimentally.

3.1.2 <u>The moment due to external hydraulic resistance forces</u>

The hydraulic forces opposing rotation are caused by friction between blades and fluid, by eddies that are shed near the rotor, and by impact of fluid particles on the meter body.

Applying dimensional analysis, this force, denoted by F_e, can be expressed as :

$$F_e = \rho D^2 V^2 \, \xi (\frac{\mu}{V \rho D} , \frac{F}{\rho D^2 V^2}) \quad \text{..............} (5.11)$$

This expression is very similar to that representing the impact force caused by a jet of fluid striking a flat surface held normal to the jet axis, viz.

$$F \quad = \quad \rho d^2V^2\phi \left(\frac{\mu}{V\rho d} \right) \quad \ldots\ldots\ldots\ldots\ldots\ldots\ldots (5.12)$$

where d = diameter of the jet, the other symbols having their usual significance. The direct solution of equation (5.12) yields simply :

$F \; = \; \rho d^2V^2$ which, for a current meter, can be approximated by $F_e' \; = \; \rho D^2V^2 \; = \; AV^2$ ....(5.13)
where A is a constant.

Now for smooth surfaces, such as current meter blades, f, in equation (5.11), is proportional to Reynolds number or

$f \; = \; B. \; \frac{V\rho D}{\mu}$, and thus the term $\frac{f}{\rho D^2V^2}$

may be written as $\frac{B}{V\mu D}$, where B is the constant of proportionality.

On comparing equations (5.11) and (5.13), it is therefore seen that F_e is made up of another component which, for a particular fluid, would be proportional to V, or $F_e'' \; = \; C.V$ .... (5.14)

Hence equation (5.11) can be represented by the sum of the two friction force components (equations (5.13) and (5.14)), i.e.

$$F_e = F_e' + F_e''$$

$$\text{or} \quad F_e = AV^2 + CV$$

The resisting moment due to the external hydraulic resistance forces may therefore be expressed as :

$$T_h = A_h V^2 + C_h . V \quad \ldots\ldots\ldots\ldots\ldots\ldots \quad (5.15)$$

where A_h and C_h are instrument constants to be determined experimentally.

3.1.3 The moment due to internal mechanical resistance forces

Internal mechanical resistance is caused by axial and radial components of bearing friction and by resistance in the contact mechanism of the meter.

At a particular free stream velocity V, the meter registers a velocity V' which is less than the free stream velocity, because of the energy absorbed by the forces of hydraulic and mechanical resistance under discussion. If this condition is considered as analogous to an actual change in fluid velocity from V to V', the corresponding rate of change of axial momentum per unit mass rate of flow = V - V' or

$$F'_v = V - V' = (V - K_s n)$$

where F_v' = force per unit mass rate flowing.

Thus the force for the total mass rate flowing through the meter may be written as :

$$F_v = D(V - K_a n) \quad \ldots\ldots\ldots\ldots\ldots\ldots\ldots\ldots (5.16)$$

where D is a constant for a particular meter and velocity. It might be argued further that at this particular velocity of flow n is constant and equation (5.16) may be expressed as :

$$F_v = D'V$$

yielding a theoretical torque of $T_v = D_0 V$ ..... (5.17)

at the velocity considered.

Equation (5.17) may therefore represent that portion of the available torque energy which is absorbed by internal friction.

This result is confirmed by equation (5.10), viz.

$T_b = C_o V \ (V - K_a n)$, which shows that, if a constant relationship exists between V and $K_a n$, the torque, or a portion thereof, may be expressed as a (constant) xV.

If the actual internal friction force is F_i, the torque caused by this force, at the same flow velocity V, may be written as :

$$T_i = F_i C_i V'$$

Where C_i is an instrument constant,

or $\quad T_i \quad = \quad F_i C_i \ (V - \Delta V)$ .... (5.18)

Now ΔV may be eliminated by writing $\Delta V = K'_a n$ and hence equation (5.18) may be expressed as :

$$T_i \quad = \quad F_i C_i \ (V - K'_a n) \quad \text{.................. (5.19)}$$

Equating equations (5.17) and (5.19) yields :

$$F_i C_i \ (V - K'_a n) \quad = \quad B_o V,$$

$$\text{or} \quad F_i \quad = \quad \frac{B_o V}{C_i \ (V - K'_a n)}$$

Thus the corresponding torque due to this force may be written as :

$$T_m \quad = \quad \frac{D.V}{V - K'_a n} \quad \text{.................. (5.20)}$$

where $D \ = \ \dfrac{B_o}{C_i}$ is an instrument constant.

The three fundamental factors involved may therefore be defined as follows :

The torque developed by the blades :

$$T_b \quad = \quad C_o \cdot V^2 \ \left(1 - \frac{K_a n}{V}\right) \quad \text{..............(5.10)}$$

The moment due to external hydraulic resistance forces :

$$T_h \quad = \quad A_h \cdot V^2 + C_h \cdot V \quad \text{.................. (5.15)}$$

The moment due to internal mechanical resistance forces :

$$T_m = \frac{D.V}{V - K_a'n} \quad \ldots\ldots\ldots\ldots\ldots\ldots\ldots\ldots\ldots\ldots (5.20)$$

When the propeller is in motion, and developing zero power, the torque and resisting moments must be in equilibrium.

Thus :

$$T_b = T_h + T_m \text{ or}$$

$$C_oV^2 \left(1 - \frac{K_a n}{V}\right) = A_hV^2 + C_hV + \frac{D.V}{V - K_a'n} \quad \ldots\ldots(5.21)$$

$$\therefore \quad C_oV^2 - C_oVK_an = A_hV^2 + C_hV + \frac{D.V}{V - K_a'n}$$

$$\therefore \quad V^2 (C_o - A_h) - C_oVK_an - C_hV - \frac{D.V}{V - K_a'n} = 0$$

Dividing by V yields :

$$V (C_o - A_h) - C_oK_an - C_h - \frac{D}{V - K_a'n} = 0$$

Solving for V gives :

$$V = \frac{C_h}{C_o - A_h} + \frac{C_oK_a}{C_o - A_h} . n + \frac{D}{C_o - A_h} . \frac{1}{V - K_a'n} \quad \ldots\ldots\ldots (5.22)$$

Grouping the instrument constants together as in equation (5.22) above, we write :

$$\frac{C_h}{C_o - A_h} = a, \quad \frac{C_o.K_a}{C_o - A_h} = k, \text{ and } \frac{D}{C_o - A_h} = m^2$$

and equation (5.22) becomes :

$$V = a + k.n + \frac{m^2}{V - K_a'n} \quad \ldots\ldots\ldots\ldots\ldots (5.23)$$

Equation (5.23) is the general characteristic equation of the current meter. When written in the form :

$$(V - (a + kn))\,(V - K'_a n) \quad = \quad m^2,$$

it represents the well-known Ott hyperbola in V^2 and n^2.

Solving the above equation for V yields :

$$V \quad = \quad \frac{a}{2} + \frac{k + K'_a}{2} \cdot n \pm \sqrt{\left[\frac{a}{2} + \frac{k - K'_a}{2} \cdot \right] + m^2} \qquad \text{.........(5.24)}$$

which is the general characteristic equation in explicit form.

In practice, the Ott propeller-type current meter has a very flat hyperbolic characteristic, which can be closely approximated by a series of tangent lines which, from equation (5.24), has the general form.

$$V \quad = \quad k_a n + A \qquad \text{..........................(5.25)}$$

where k_a and A are instrument constants which have to be determined from calibration tests. The so-called hydraulic pitch, k_a, represents instrument geometry, while A, usually referred to as the 'residual velocity', defines the internal meter friction forces. Current practice is to determine k_a and A by towing the meters through still water.

3.2 An analysis of the factors affecting the functioning of current meters.

3.2.1 Rating by towing through still water

The characteristic equations of a current meter, as derived in the previous section, are evaluated by towing individual meters, or a group of meters, through still water in a calibration tank. The two methods employed are tangent rating, i.e. straight-line towing in a rectangular tank, or rotary rating, i.e. towing along a circular path described by a rotating beam.

The flow patterns associated with the moving of a meter through still water are quite different from those existing when a current meter is held stationary in a flow field where oblique currents and eddies, rather than parallel filaments, are encountered.

It will be shown later that a propeller-type current meter tends to over-register in turbulent flow, while oblique currents cause underregistration. The difference, therefore, between the flow structure when calibrating and that prevailing in practical application, constitutes a source of unknown error in the rating characteristics obtained by towing. Evaluation or elimination of this error remains a problem.

Attempts have been made to devise alternative methods of calibration e.g. towing a meter with and then against a steady current in an open channel, as suggested and investigated by Lindquist in 1924.(63) In the lower velocity ranges, and under more or less ideal conditions, this method gave results almost similar to those obtained from still water ratings. The effects at higher velocities and under different levels of turbulence have not, to the author's knowledge, yet been investigated.

It is indeed probable that, irrespective of turbulence, meter operation would be affected by the nature of the velocity profile at the meter position. The effect of angularity is dealt with later, but it seems correct to state that the difference in angle of incidence of a velocity vector encountered under conditions of towing and flowing, respectively, would greatly influence the torque developed and hence the characteristic equation (See equation 5.5).

West, in a discussion on a paper by Benini, (11) pointed out that, during towing, a V-crested velocity distribution would presumably exist in front of the meter, and turbulent eddies would be shed beside and behind the propeller. When the meter is stationary, on the other hand, the propeller would modify the existing natural velocity profile of the flow, thereby altering the incidence of the local velocity vector which would differ appreciably from that for the towing condition.

It would therefore appear necessary to start thinking along the lines of developing possible methods by which not only studies on current meter operation and performance, but possibly all current meter ratings could be carried out in flowing fluids instead of in a medium at rest. This aspect will be dealt with later.

3.2.2 The effect of the supporting current meter frame

In modern current meter practice, the supporting frame is constructed as lightly as possible to minimize blockage and interference effects, while streamlined sections are usually adopted to prevent undue disturbance of the natural flow pattern. Framed structures and sections, for laboratory and field applications, should be similar to those used in the rating tests.

Thus far few references to experiments are to be found in the literature,[14] and in these only the effect of the supporting frame on meter performance has been studied; the mechanism of the effect seems to have been neglected.

At a recent symposium on flow measurement, Serpaud and Coffin [14] reported results of model experiments associated with field measurements on a large Kaplan turbine; these gave flow-rate values 7 to 8 per cent below those predicted according to Hutton's [28] scale-up formula. The authors suggested that the support frame used in the field tests had caused a local change of the velocity profile, which turned out to be a flow retardation. This paper focused attention, for the first time, on the mechanism of the support frame disturbance. The authors submitted that there was some form of retardation at the elevation of the horizontal frame together with a general acceleration on either side of it.

In the discussion of Reference 14, Chaix reported a similar tendency in results obtained in Geneva : an isolated rod carrying six current meters in a rectangular conduit registered velocity approximately 1 per cent below the value obtained in the same section using a grid of six vertical rods. As pointed out by Chaix, this effect could be explained by two-dimensional potential flow theory, which reveals that stagnation points would be formed at the supporting rod. This will be discussed presently.

In the same discussion, Prof. Gerber reported that experiments in a rectangular section, carried out in Switzerland, with supporting rods differing in section and in number, and carrying up to forty-five meters at a time, revealed velocity errors of up to 6 per cent; he found that the error was not dependent on the rod section but on the number of rods in the conduit section and, to a second order, on the number of current meters on the rods. He stated that further testing was in progress to verify the above findings. The author is of the opinion that the reported independence of the error on rod section is a debatable point which requires further investigation.

Winternitz,[14] on the other hand, reported results of aerodynamic model tests carried out at N.E.L. in connection with current meter measurements of flow in penstocks. The findings contradicted the above hypothesis and its related experimental results. In these investigations, undertaken in the N.E.L. windtunnel, the current meter support consisted of a cross with four to eight radial arms, in the plane of measurement. The blockage, it is argued in this case, caused a 'venturi effect' which clearly was initiated some distance upstream from the metering plane because the acceleration could not occur instantaneously in the plane of the cross. The current meters would therefore over-register, i.e. indicate larger rates of flow than the actual. The over-registration was found to be directly proportional to the blockage, irrespective of whether the support consisted of a multi-arm cross or a single member.

This hypothesis, directly opposed to that enunciated by Serpand, Coffin and others, (14) was, according to Winternitz, confirmed experimentally at N.E.L. The validity of transposing the findings on the model tests, reported in Reference 14, to prototype conditions is not relevant here.

The author will attempt to analyse the results of the different experiments on interference effects. As stated earlier, a single horizontal cylindrical bar carrying current meters in, say, a flume or a pipe would form a horizontal stagnation 'line'. The fluid would tend to decelerate at the particular elevation of this 'line' and the upstream reach of this effect from the 'line', would produce a more slowly flowing zone enveloping the projecting current meters. The result would be under-registration.

On either side of the horizontal bar, however, there would be acceleration due to the blockage effect, and at those particular elevations, other than the metering one, increased velocities would be recorded by, say, a pitot tube. This increase of velocity need not be imagined as ins[illegible] at the particular section or elevation. The conditions could be considered as analogous to a form of locally increased shear flow, in that a flow layer at the bar elevation is gradually retarded while the two adjacent layers, above and below the bar, are gradually accelerated - hence the distorted velocity profile.

If this single bar is now replaced by a grid of several horizontal bars, or by a cross, it can be shown, by applying two-dimensional potential flow theory, that the upstream reach of the decelerated zone is decreased considerably, so that the projecting propellers would probably be located outside this zone. Under these conditions the degree of under-registration would of course be less.

The author further submits that the above conditions would obtain for a bar of circular cross section and particualr dimension. The mechanism of the effect suggests that the effect itself would be controlled by the type of section, its size and the Reynolds number.

The marked influence reported in Reference 14 is probably due to the outsized circular section used as current meter support. Coffin, indeed, categorically states : 'In this particular case, the question of strength of materials was considered more important by the designers than the precautions which would have been taken by the fluid dynamicist'. He concludes with the remark that they (the authors) 'wanted to give their colleagues the successive images of the velocity profile deformations with the displacement of an over-dimensioned frame'.

Thus, when using light streamlined strut sections in a current meter supporting frame, the drag coefficient over the Reynolds number range under consideration would decrease from approximately 1 (for circular cylinder) to 0.1 for an air-foil strut section. Here the formation of a stable horizontal stagnation 'line', on the thin edge of a strut, would be very unlikely in a flow field and consequently the deceleration zone would be prevented or minimised. The only other factor which now enters the argument is that of blockage which, as pointed out earlier, would cause an over-registration due to gradual acceleration at the metering section, as reported by Winternitz.

In the light of this analysis, Prof. Gerber's remark, referred to earlier, that the frame-error was independent of the shape or size of the supporting rod needs further investigation and clarification.

A detailed study of this factor based on pitot-static or pitot-wall static traverses over cross-sections with frames of various designs would be of value. Relatively small probes could be employed to determine absolute values of point velocities at the grid or frame position, while velocity profiles at sections immediately before and after the metering plane could be investigated under various flow conditions and frame/meter configurations.

3.2.3 The effect of current meter positions relative to solid boundaries and adjacent meters

To measure velocities as accurately as possible by means of current meters, it is essential to take measurements at a sufficiently large number of points in the cross-section of a pipe or flume and, where steep velocity gradients exist, e.g. near solid boundaries, the density of measuring points must be adequate.

Optimization of meter positioning in a cross-section will be dealt with later, but irrespective of position, the number of meters required and the presence of solid boundaries create problems of proximity interference effects.

The author could not find in the literature evidence of extensive study of this factor. Staus [64] and Henn [65] reported results of some earlier investigations. According to Staus, a propeller-type current meter records an error of -0.8 per cent near the bottom of a flume and a -1.1 per cent error near a wall, these errors being independent of the absolute velocity.

Tests carried out by Ott [66] revealed different results, in that the negative errors increased with increasing velocity. Meters near the bottom showed errors of -1.2 per cent, while errors of -2.1 per cent were registered by meters near a wall, both at a velocity of 2.5 m/s. Ott also found that there was no significant interference between two meters in the velocity range 0.1 to 0.8 m/s.

According to Benini, [11] research carried out at the Institute of Hydraulics in Belgrade yielded results even more at variance with the foregoing; in the velocity range 0.5 to 4.5 m/s, meters near the bottom registered as much as 1.7 per cent too low at the maximum velocity.

Tests on three similar meters, spaced at 3 cm between peripheries of propellers, showed that the middle meter tended to record low readings; here, however, the errors were a maximum at the low velocities, viz. 2.4 per cent at 0.5 m/s as against 0.8 per cent at 4 m/s. Agreement or even an approximate trend is therefore non-existent. This uncertainty about proximity effects is also reflected in the several international code specifications.

The French code stipulates a minimum distance from wall to propeller periphery of 3 cm. The German Code, on the other hand, specifies minimum distances in terms of propeller diameter D; viz. the minimum distance between meter axis and wall should be 0.75 D, while the distance between adjacent meters should not be less than 1.2 D. (67)

Recent experiments on proximity interference were carried out at Padua University by Prof. Benini (11) who towed pairs of current meters, suspended both vertically and horizontally, through still water. Interference-free datum values were established by towing adjacent current meters 60 cm apart, and a single meter was towed at an identical distance from a wall. The depth of submergence was 50 cm. The results were disappointingly inconclusive as discrepancies attributable to inherently unavoidable experimental error masked any effect of proximity interference. He submitted that, within the range investigated, the possible effect would not exceed 0.2 to 0.3 per cent. This result was clearly in direct contrast to those reported by other investigators.

The results discussed so far seem to indicate that experimenters have concentrated on the experimental effect of proximity interference with complete disregard for the underlying physical mechanism.

The author is of the opinion that the root of the problem is in the method of towing current meters through still water, and this hypothesis is now analysed.

The manner in which one current meter, or a solid boundary, can interfere with the operation of an adjacent meter may be visualised in broad outline by recognising that the 'interference' results from an alteration in the natural flow pattern at or near the meter. When there are two adjacent meters the flow past one will interfere with that through the other. The flow direction at exit from the blades of one current meter is such as to induce angular components or artificial turbulence in the flow field of its neighbour; the velocity distribution induced (towing) or natural (flowing) can be so distorted by the proximity of one meter to another that the meter propeller is not subjected to normal velocity vectors.

The picture is identical when a current meter is operated close to a wall. Here a boundary-layer exists which deflects currents obliquely into or away from the flow field of a meter. The flow pattern may also be altered when the flow exiting from the blades is reflected from the wall itself in the form of turbulence. In brief, the structure of interference alters the true velocity profile.

The next point to consider is : how do conditions of towing and flowing affect this interference mechanism?

When a horizontal frame supporting several meters is towed through still water, there exist between the meters, zones of relatively inactive liquid forming barriers between the active fields at and near the propellers.

This is particularly so if streamlined strut sections are used for the support frame, because the propellers are usually located well upstream of the frame. Oblique flow from the propellers thus impinges on these fluid partitions to either side of a particular current meter. Flow which is diverted around the meter bodies is also shed into these inactive barriers. Depending on the conditions, both types of flow are either let through into the active flow field of the adjacent current meter or damped.

When a single meter is towed in still water near a wall, a similar barrier or partition is formed between the active propeller zone and the wall, and this tends to damp diverted and propeller flow components.

When meters are placed in flowing water on the other hand, the picture differs markedly. There are no inactive fluid barriers between the propellers and the diverted flow components, and propeller flow can either be diffused in the flow zones between the propellers, or be converted into turbulence at or near the adjacent propellers. A single meter near a wall in flowing water would have no inactive fluid barrier between itself and the wall. Here, diverted and propeller flow components would probably be deflected from the wall as a form of turbulence near the propeller.

The author submits that if in the towing situation the fluid partitions act as damping zones, adjacent meters would be protected from interference components, so that normal proximity interference effects would not be detectable. This hypothesis could possibly explain the results reported by Prof. Benini.[11] Although the errors found by Ott [66] seem rather high, the trend of his results falls into line with this theory in that the interference error increased with velocity whereas Ott could not detect any proximity interference effects between two current meters in the velocity range 0.1 to 0.8 m/s.

The analysis therefore suggests that it is not correct to evaluate interference effects by towing experiments and then apply the results to current meters placed in a flowing fluid.

Further and more intensive research appears to be imperative, and it is most encouraging to learn, according to Prof. Gerber [11] that some of the factors analysed above are to be investigated in detail at the E.T.H. in Zurich, as well as by the International Current Meter Group.

3.2.4 The temperature and pressure effect

Temperature changes and high line pressures can affect current meter operation in that a change in the viscosity of the lubricating oil can modify the internal friction forces and hence the value of A in the rating equation (equation 5.25). High line pressures, sometimes encountered on hydro-electric plants, can also change the viscosity of the protecting oil in that water can be forced into the meter bearings to mix with the oil.

In a recent paper on the influence of this factor Coffin [13] found that water temperature and oil viscosity had a considerable effect on rating characteristics. He showed that the variation of A, the 'residual velocity', was a function of oil viscosity and temperature of the water in which current meters were placed. These functional relationships were presented graphically.

The conclusions arrived at were that, for current meters filled with Frigolene A oil, the variation of Δ was almost proportional to temperature changes, and that the mean comprehensive rating formula within the range $4 \leq n \leq 11$ could be stated as :

$$V = K_a n + \Delta - \frac{t^oC}{1125^oC} \quad m/s$$

where 't' is the temperature of the water.

These results cannot be deemed to be a satisfactory basis for comparison because several groups of current meters were used with different brands of lubricating oil.

Discussing Coffin's paper, Böhm-Raffay contradicted the conclusions and reported that in numerous calibration experiments conducted in Vienna during the last ten years, in water temperatures varying from 50°C to 15°C, no effect of water temperature on the rating characteristics was detected. In these experiments, Ott V-type current meters lubricated with the manufacturer's oil were used.

In tests carried out at N.E.L. on 50 mm Ott current meters in a towing tank, Winternitz [13] found that the rating equations determined with pure oil and with a water/oil mixture in the meter bearings were identical. This result implies that both high mains pressure and temperature variations are unlikely to affect calibration because it would require a considerable temperature change to bring about a viscosity equivalent to that of a water/oil mixture.

Robson [68] investigated this factor very thoroughly insofar as it affects a type A low-velocity current meter used by the U.S. Geological Survey. The results show that within two decimal places the accuracy of ratings in the velocity range 0.15 to 7.0 ft/sec is not altered by change of water temperature from 36.9 to 62.5°F.

The mechanism of the modification of internal friction by viscosity and/or temperature changes, however, is not simple; often complex inter-related influences, such as primary thermal effects on friction, may require consideration. Available experimental data indicate that this effect is not serious for the Ott-type current meters lubricated with the maker's oil, but this does not necessarily hold for other current meters of different design. It would therefore seem advisable to investigate possible temperature and pressure effects separately on different types of current meters and, where necessary, to establish correction factors for various conditions of metering. It is known that current meters calibrated in Europe are employed in countries of tropical climate, with possible introduction of unpredictable errors

To overcome the difficulty, it may be necessary to design current meters having pressurized floating bearings.

3.2.5 The effect of waiting periods in rating tests

Irrespective of the inherent errors associated with rating current meters by towing through a still fluid, calibration errors can also result when waiting periods between consecutive towing runs are too short. Random currents induced in the towing tank during an earlier run, affect the rotational speed of a towed meter and hence influence the rating. Theoretically, the error is cumulative because with every consecutive test run fresh disturbances are superposed on decaying ones. Waiting periods should therefore be rather too long than too short and should lengthen with increasing towing speeds as the rating proceeds. The degree of persistence of disturbances depends upon the dimensions of the towing tank and differs along the length of the tank. Being dependent on rating and waiting times, calibration costs are high and it follows that it is important to determine accurately the required waiting intervals for a particular towing tank at various rating velocities.

In the absence of a reliable guide, differing standards are probably applied. Benini, (11) in his experiments, allowed a 'normal' interval of five minutes between one run and the next. Apart from the fact that the interval was kept constant over a speed range of 0.5 to 3.5 m/s, it seems to be totally inadequate.

In Vienna, Fr. Böhm-Raffay [11] showed a more realistic approach than Prof. Benini. He found that to reduce the scatter to within approximately ± mm/s, over a towing speed range of 0.5 to 4 m/s, waiting intervals of ten minutes to more than one hour were necessary. Attempts to reduce these intervals simply widened the scatter. Since the tanks at Vienna and Padua are almost identical, the accuracy of Prof. Benini's results must be questioned.

Waiting times allowed by the Swiss Federal Administration in their towing tank vary with towing speeds but are normally from 30 to 45 minutes.

In rating tests carried out by Robson [68] to determine temperature effects, a constant waiting interval of 45 minutes was allowed over a speed range of 0.15 to 7 ft/sec. The tank dimensions, however, were not given.

In calibration experiments undertaken by the author at the National Physical Laboratories (N.P.L.),[69] to be dealt with later, waiting times varied from five ... 15 minutes but the towing tank was approximately twice the size of those at Vienna and at Padua.

It would seem that the waiting time aspect could be investigated thoroughly by performing velocity traverses at various sections along a towing tank at different time-intervals following completion of a return run. Sensitive miniature current meters, as developed by Dedow [70] at Wallingford, could be employed for the purpose. The results would yield a picture of the variation with time of disturbance intensities at different cross-sections for different 'disturbance runs', and these could be compared with the actual scatter on velocities obtained from subsequent ratings at corresponding times. For particular tank dimensions, minimum waiting intervals for different towing speeds could then be established to meet velocity scatter tolerances.

3.2.6 The effect of submergence

When a current meter is too shallowly submerged, free surface disturbances caused by wind or by the supporting frame can be transmitted to the propeller, thereby affecting the rating characteristics. The author could not find literature in which experiments on this factor specifically are described.

Benini, [11] in his experiments on proximity

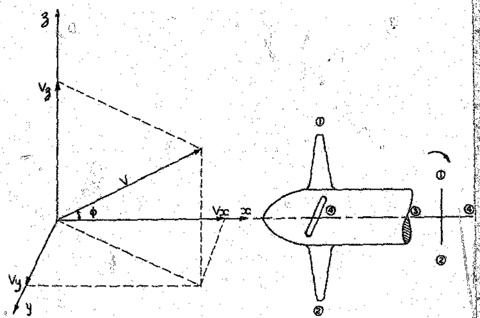

FIG. 5·2 CURRENT METER SUBJECTED TO OBLIQUE FLOW
(DIAGRAMATIC)

effects, adopted a depth of 50 cm. In the discussion of this paper, this depth was queried by Winternitz who thought that surface disturbances could probably still have effect at that depth. This point of view is difficult to reconcile with the fact that, after several trial runs to establish a reasonable and practical interference-free depth, Winternitz and the author adopted a minimum submergence of 14 inches for their rating experiments at N.P.L. (69)

Minimum depth must, of course, be dictated by such factors as : maximum towing speed, location of the tank (indoor or outdoor) and the degree of surface disturbance caused by the supporting frame.

3.2.7 Oblique flow effects

The axis of rotation of a current meter is usually aligned parallel to the axis of the conduit in which measurements are to be made. In many practical installations, however, flow is oblique to this axis but evaluation of the component of velocity parallel to the conduit or meter axis is desired, not the absolute value of the local oblique velocity. In Fig. 5.2 this component is given by V_x, where

$$V_x = V \cos \emptyset$$

It has been determined experimentally that for oblique flow, the velocity registered by the current meter is always less than the axial component V_x. This discrepancy was found to increase with increasing $\emptyset$, the increment being smaller for a blade than for a screw-type rotor. The ideal current meter should therefore accurately record the instantaneous value of $V\cos\emptyset$, as an average value of velocities over the area swept by the propellers, for as large a range of variation of $\emptyset$ as practicable.

To gain an appreciation of the effect of oblique flow, its mechanism in relation to the operation of a current meter will now be analysed. Fig. 5.2 shows diagramatically a four-bladed current meter subjected to a mean oblique velocity vector V. In the theoretical analysis at the beginning of this section, it was shown how the torque due to the axial velocity component V_x can be calculated. Here, however, the analysis is complicated by the additional effect of the radial components V_z and V_y when the blades are in positions perpendicular or parallel to these directions. In the position shown in Fig. 5.2, it is evident that blades 3 and 4 are perpendicular to V_z and parallel to V_y, while blades 1 and 2 are perpendicular to V_y and parallel to V_z. The parallel position does not readily lend itself to mathematical analysis. A feasible mathematical model can, however, be applied when the blades are perpendicular to the radial components. The effect of V_z on blades 3 and 4 will therefore be considered.

If the meter rotates in a clockwise direction, it is evident that as soon as blades 3 and 4 move away from the six o'clock position the radial component, V_z, tends to produce a driving torque on blades 3 and 1, accompanied by a resisting torque on blades 4 and 2. This effect will be a maximum on blades 3 and 4 when they are in the horizontal position, and non-existent on blades 1 and 2 when in the corresponding vertical position.

Fig. 5.3 shows the vector diagrams (schematically) for blades 3 and 4 in horizontal position. Triangle ACE represents the diagram for any of the blades when subjected to the axial component V_x, while triangle ABE and ADE are respectively the vector diagrams for blade 4 (being resisted) and blade 3 (being driven) under the influence of the radial component V_z. It is seen that as the meter rotates the direction of the velocity at entrance to the blades varies according to the positions V_r, V_{r2}, V_r, V_{r1} for alternately vertical, horizontal, vertical, and again horizontal blade positions.

If the current meter is to rotate at a speed determined by V_x only, the question arises : how can the

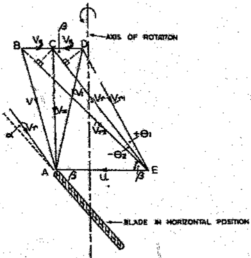

FIG. 5·3 VECTOR DIAGRAM SHOWING EFFECT OF RADIAL COMPONENTS IN OBLIQUE FLOW

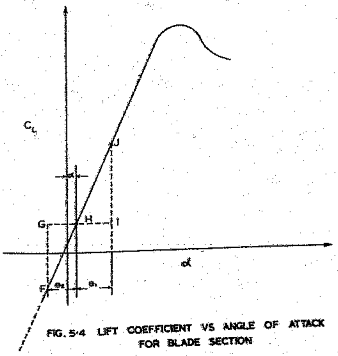

FIG. 5·4 LIFT COEFFICIENT VS ANGLE OF ATTACK FOR BLADE SECTION resisting and driving torques on blades 4 and 3 respectively be balanced under the above conditions of flow, neglecting for the moment the effects on the other blades?

The fundamental torque equation may be expressed thus :

$$T = \int_{r_i}^{r_o} C_L \rho (V^2 + U^2) \,\&\, r \sin\beta \, dr$$ (see development of equation 5.5). For a particular blade design and pitch angle, β, the torque is associated with a lift coefficient C_L and the square of the relative velocity V_r^2 ($V_r^2 = V^2 + U^2$). The effect of C_L may be analysed as follows :

Fig. 5.3 shows that the angle of incidence on blades 4 and 3 varies from $(\beta - \theta_2)$ to $(\beta + \theta_1)$. Consequently the angle of attack, α, will vary over the range $-\theta_2$ to $+\theta_1$. It is also evident that :

$$\operatorname{Tan} \theta_1 = \frac{V_z \sin\beta}{\sqrt{V_x^2 + U^2} - V_z \cos\beta}$$ and

$$\operatorname{Tan} \theta_2 = \frac{V_z \sin\beta}{\sqrt{V_x^2 + U^2} + V_z \cos\beta}$$

Thus, $\theta_1 > \theta_2$, the difference depending on the angularity of flow. In Fig. 5.4, the effect of this change in C_L shows that the amount by which the lift coefficient on blade 3 is increased, i.e. I J, is approximately equal to the decrease in C_L on blade 4, i.e. F G. If the angle of attack, α, at which the blade normally operates is increased (Fig. 5.4) a variation of this angle over the above range would have an identical effect on the lift coefficient, provided the linear portion of the C_L vs α curve is applicable. Thus, the difference in torque due to this small second order difference in lift coefficient is negligible, the resultant being a very small driving torque (I J $\geq$ F G).

The effect of the difference between the magnitude of V_{r1} and V_{r2} presents a different picture. From Fig. 5.3, these values can be written approximately as :

$$V_{r1} = V_r - V_z \cos\beta \quad \text{and} \quad V_{r2} = V_r + V_z \cos\beta$$

Thus, according to equation (5.5), the resisting torque on blade 4 is greater than the driving torque on blade 3, the difference being proportional to $V_{r2}^2 - V_{r1}^2$ where

$$V_{r2}^2 - V_{r1}^2 = 4V_r V_z \cos\beta,$$

whence $\sigma T = KV_z \cos\beta \sqrt{V_x^2 + U^2}$ ....(5.26)

where K is a constant.

Similar analysis would show that the effect of V_y on blades 1 and 2, in the six o'clock position, produces a retarding torque on blade 2 that is greater than the driving torque on blade 1.

In addition to the foregoing effects, the radial flow of V_y, when blades 3 and 4 are in a horizontal position, together with the radial flow of V_z, when blades 1 and 2 are in a vertical position, would cause a drag force on these blades possibly resulting in under-registration.

It is evident that, due to the resisting effects of the radial flow components, a current meter should under-register in oblique flows as experimental measurements indeed show.

In equation (5.26), V_z and V_x are determined by the angularity and magnitude of the velocity of flow. The error of under-registration must, therefore, be minimized by selecting a large value for β and by keeping the speed of rotation, U, as small as practicable. This conclusion is probably worthy of further investigation, especially under conditions of strongly oblique flow.

If pressurized liquid, or floating bearings, are used in current meters, internal mechanical resistance will be minimized; speed of rotation can if necessary be checked by magnetic braking. For such a meter the calibration equation would of course change for different degrees of braking, and the meter would have to be calibrated accordingly. This is merely a broad suggestion prompted by the idea possibly of measuring torque developed instead of speed of rotation, with the object of minimizing the errors analysed above.

A classical method adopted by Lindquist [71] in 1927 to minimize these errors was to shroud the propellers of a current meter in a cylinder which caused the flow to be diverted into the propeller circle to ensure that it would be proportional to Cos ϕ. Such a meter followed the cosine law to flow angles of more than 30^o.

Cup-type meters register velocity inaccurately in oblique flow. Screw-type current meters yield more reliable results because they measure the projected velocity to a higher accuracy. According to Kolupaila [9] a meter with a 'component runner' measures a projection of the velocity, according to the cosine law, for oblique flow angles of 45^o and more.

The foregoing analysis of the behaviour of a current meter in oblique flows once more illustrates the difference between this type of flow and that encountered under normal conditions of rating.

3.2.5 The effect of turbulence

Under turbulent conditions, successive velocity vectors at entrance to the propeller blades may fluctuate rapidly in magnitude causing variation in torque (equation 5.5). These vectors may also frequently strike the blades at oblique angles of possibly rapidly varying magnitude. Another phenomenon of turbulence is the non-uniformity of velocity distribution over the area swept by the propeller blades. The effect of these factors on the speed of rotation requires examination.

The scale of turbulence appears to be an important factor. If the diameters of the fluid masses composing the turbulence are larger than the diameter of the meter, the propellers would be subjected to a type of homogeneous flow field in which it would record a series of pulsations about the average value. On the other hand, in small scale turbulence, with eddies small in relation to chord length of the blades, small pulsations might be masked and the rotor velocity might be constant.

In practice, one would expect the scale of turbulence to vary in size from very much larger to very much smaller than the meter diameter, and the meter will be subjected to a spectrum of turbulence difficult to analyse. If it be assumed that the mean velocity parallel to the axis of rotation is V_x and the instantaneous turbulent fluctuating components in this direction are v_1, v_2, v_3 etc., neglecting at this stage the other two components at right angles, the torque and hence the speed of rotation will be dependent upon the square of the velocity V_x (equation 5.5); the ideal meter would rotate at a speed proportional to the instantaneous average velocity through the meter area. However, due to turbulence, the velocities at different points in the meter circle depart from the true average, and the torque will now depend on the mean square value of these different velocities in the meter area instead of on the square of the mean velocity. Thus, if these velocities are written as :

$$(V_x + v_1),\ (V_x + v_2)\ \ldots\ldots\ldots\ldots \text{ and } (V_x + v_n)$$

then $$\sum_1^n \frac{(V_x + v)^2}{n} = V_x^2 + \frac{2V_x}{n}\sum_1^n v + \frac{\sum_1^n v^2}{n},$$

which is clearly greater than V_x^2. Therefore, fluctuations parallel to a meter axis cause a tendency to over-register.

The transverse turbulent components, which were neglected in the above analysis, can be considered as altering the magnitude and direction of the axial velocity, V_x, at entrance to the blades. If V_x is slightly increased, over-registration would result, as shown above, whereas a directional change would give rise to a radial velocity component which, on one blade assists rotation while retarding it on the diametrically opposite blade. This is identical to the effect of radial components caused by oblique flow components dealt with in the foregoing sub-section, where it was shown that the resisting torque on one blade is greater than the driving torque on the other. The transverse components therefore cause under-registration.

The extent to which over-registration masks the under-registration is not known. Kolupaila, (9) however, pointed out that the mechanism of pulsating flow appears more as an irregular variation in the general direction of flow rather than as a change in its magnitude. If this hypothesis is accepted as approximately true, the axial fluctuating components would cause over-registration, as shown, while the tranverse components cause under-registration only. Over-registration is thus more pronounced than under-registration. According to reference (9), current meters may be quite unsatisfactory in strongly pulsating flows, over-registering sometimes as much as 2 per cent.

In his discussion of reference (9), Chaix reported experiments carried out in collaboration with Sulzer Bros. and the Swiss Federal Hydrological Institute in

Berne: The turbulent component normal to the runner axis of a component-type current meter was investigated by oscillating the meter in a vertical plane in running water. The meter registered up to 2 per cent higher than when the instrument was at rest in the same flow. Experimental results for the normal runner and for the effects of the other components of turbulence are not yet available.

Owen, in the same discussion, remarked that he had found a vane anemometer to over-register in pulsating flow by an amount proportional to the square of the amplitude of the pulsations.

Thus, analytical conclusions and the results of current experimental work are in agreement on the effect of the turbulence factor. The magnitude of the error resulting from turbulence for various types of current meters needs further attention.

The factor of still-fluid calibration is seen to re-enter the picture. High accuracies cannot be expected when normal rating characteristics are applied to measurements of velocity in strongly turbulent flows.

3.2.9 The effect of steep velocity gradients

When a meter propeller circle is cut by a steep velocity gradient, there arises a centre line displacement effect analogous to that observed when a total pressure probe is placed in a steep pressure gradient.

Because of the velocity gradient, for example near a solid boundary, the blades of a current meter nearest to the boundary would be subjected to flow velocities lower than those diametrically opposite. Consequently the average velocity operating on a boundary-side blade would be less than that for a blade on the opposite side. It is therefore evident that the average velocity, which the meter tends to register, does not pass through the meter centre line but through a point displaced from the centre line towards the higher average velocity. The weight of this factor would depend on the velocity gradient and on the current meter and pipe sizes; a small meter in a large pipe would be inappreciably affected. For air flow having a normal turbulent velocity profile in a pipe, Owen [72], [9] found that the diameter of an anemometer circle had to be less than one-sixth of the pipe diameter to keep the error due to this factor below 1 per cent.

In his discussion of reference (9), Prof. Gerber referred to a doctoral thesis at E.T.H. in Zurich where it was found that normal three-bladed current meters showed, in large penstocks, velocity profiles different from those in small laboratory pipes at identical Reynolds numbers. This was probably attributable to the displacement effect, but it would be of interest to know what the result would have been had current meters of different sizes been used in the same pipe or penstock at identical Reynolds numbers. The wall proximity and turbulence effects in a large penstock would surely differ for the same current meter from those in a small laboratory pipe.

The experimental procedure for studying the error arising from this factor is complicated by the necessity to isolate proximity and turbulence effects near a solid boundary where the velocity gradient effect would be a maximum.

It would seem that attempts to isolate these errors at this stage would be fruitless; a calibration method in which some factors are allowed to combine and be reflected in the rating characteristics would seem to be a more promising alternative.

A final question of interest is whether attention has been given to the possible weight of the velocity gradient effect when specifying minimum sizes of current meter in pipe flow measurement associated with power test codes.

3.2.10 The effect of inertia

In pulsating flow, a current meter response-lag depends on the rate of velocity fluctuation and the inertia of the meter including the virtual mass, which can be considered as the mass of flowing fluid causing propeller motion. Meter response can be expressed (73) as :

$\Delta T = I \frac{d\omega}{dt}$ from which it follows that, for rapid response, the torque developed by a small change of velocity should be large. Thus, the moment of inertia and bearing friction should be a minimum.

Clearly, in this respect propeller-type current meters are superior to cup-type; moreover rapid-fluctuating velocities are not registered by a current meter as its tendency is to integrate the velocity with time.

3.2.11 The effect of Reynolds number

In a foregoing section the author drew attention to a possible effect of Reynolds number on meter characteristics when the blade boundary layers trigger from laminar to turbulent conditions; this critical Reynolds number depends on the blade shape and on the ambient turbulence. According to reference (73), the break sometimes encountered in a rating curve could probably be attributed to this boundary-layer transition.

The possible effect of this factor on overregistration in turbulent flows above the critical Reynolds number demands investigation.

3.2.12 <u>The effect of number and location of meters.</u>

Normally a pipe cross-section is divided into concentric annular rings of equal area, the innermost being a circle. Meters are positioned on concentric circles which bisect each ring into two equal areas and the arithmetic mean of the velocity readings is taken as the average flow velocity through the cross-section.

The number of gauging points, their radial positions, and the methods of evaluation are detailed in standards of flow measurement and in power test codes in accordance with empirical rules. In the German standards of 1957 there appears a table of these positions.

To measure accurately, as many meters should be employed as can be practicably accommodated. Proximity interference effects between meter and wall and between adjacent meters, however, enforce a limit. The number of current meters and their positions in a cross-section would be dictated by proximity effects, pipe diameter and roughness factor, and the velocity distribution.

With this in mind, workers (74) at N.E.L. developed a novel method of numerical integration of velocity profiles in pipes. This 'Log-Linear Law' method is based on determination of the exact mean of the function :

$$V \quad = \quad A + B \log \left(\frac{y}{D}\right) \quad + \quad C\left(\frac{y}{B}\right) \quad \ldots\ldots\ldots\ldots (5.27)$$

where V = point velocity;

y = distance from pipe wall;

D = pipe diameter, and

A, B & C = constants for a given velocity profile having dimensions of velocity. It can be shown that, for a particular velocity distribution, the original Nikuradse (75),(76) equation for fully developed flow in rough pipes can be written thus :

$V \quad = \quad A + B \log \left(\frac{y}{D}\right)$, from which Ross and Robertson (77) deduced equation (5.27) for the velocity distribution is incompletely developed flow.

From the above equations, the calculations for the meter positions are based on the assumption that in each anulus in the pipe cross-section two positions exist where the average of two velocity readings is exactly equal to the mean velocity of flow through that anulus, provided that the velocity profile can be defined adequately by the above equations. The mean flow velocity for a cross-section would then be identical to the mean of the individual measurements.

This method is dealt with in detail in reference (74) where the calculated positions for 3, 4, 6, 8 and 10 meter positions per diameter are tabulated.

The four-point log-linear rule when applied to forty fully developed velocity profiles gave mean relative errors of less than 0.5 per cent, while the standard ten-point tangential rule yielded errors of +1 per cent throughout. This numerical method has since received further attention at N.E.L.[78] and has proved to be superior both in accuracy and in computation time to graphical planimetering and to the standard numerical integration methods specified in the standards and power test codes.

It was recently suggested by Prof. Kolupaila[9] that a velocity distribution law could be assumed and meter positions computed such that each is represented by an equal area under the v vs r curve. This is fundamentally similar to the log-linear method.

Thus, in deciding on the number and positions of meters, prescriptions laid down in the standards for flow measurement and in power test codes should not be followed blindly. The log-linear method will result in improved accuracy for fewer metering positions, even for distorted velocity profiles.

3.2.13 Recording, servicing, and care

Recording methods and instruments should be accurate and reliable. In the light of factors discussed it seems advantageous and logical to apply numerical methods of computation with digital recording, rather than graphical evaluation of chronograph records.

Completely transistorised automatic recording gear for rating, laboratory and field application has been developed at N.E.L. and is described in references (69), (79), (80), (81), (82) and (83). This equipment ensures the most convenient and accurate recording known to the author.

According to the theoretical analysis, the fundamental requirements for constant measuring characteristics are unvarying blade shape and consistent internal friction resistance. This can be realised by frequently checking the blade shapes against two-piece plaster moulds, and by regular and meticulous meter servicing.

Whereas errors arising from poor recording, servicing and care can be controlled, evaluation and/or control of complex interrelated error-effects due to the other factors analysed thus far define the challenge which will have to be met if, in future, velocity measurements by current meter are to be in error by less than $\pm$ 1 per cent.

4. CURRENT METER CALIBRATION AND APPLICATION

Current meters are among the standard means of flow measurement in the Republic of South Africa. These instruments are used extensively by workers in universities, research establishments, the Department of Water Affairs, the Chamber of Mines, consulting engineering organisations to mention only a few. Measurements of unknown accuracy are being used in research and design because not a single university or other research establishment in the Republic possesses facilities for calibration of current meters. Invariably the manufacturers' ratings are adopted and instruments are seldom returned to the makers for recalibration.

At N.E.L., research on current meters was initiated with the object of improving existing calibration and application techniques. The author was associated with rating experiments carried out at N.P.L. and Admiralty Research Laboratories (A.R.L.) in London and

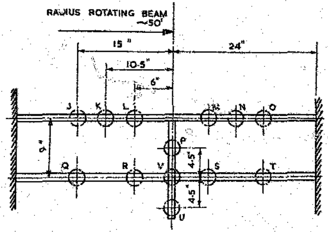

DOWNSTREAM VIEW

J 9155			Q 9162	
K 9156			R 9163	
L 9157		P — 9161	S 9164	
M 9158			T 9165	
N 9159			U 9166	
O 9160			V 9167	

FIG. 5.5 CURRENT METER POSITIONS ON SUPPORT FRAME

subsequently with further work at N.E.L. on a 20-inch calibration line, and with field measurements at a hydro-electric scheme at Kinlochleven. These experiments led to the development of novel methods featuring automatic recording gear, electromagnetic counters, electronic control and recording equipment, and improved techniques of calibration and evaluation. This work and subsequent refinements in instrumentation are described in detail in references (69), (74), (78), (79), (81), (82) and (83). The section which follows, contains a discussion of the methods adopted and results, which emerged from the factor analysis first described.

4.1 Test facilities and experimental procedure

4.1.1 Calibration experiments

Two tangential test series were conducted at N.P.L. and one comparative series was carried out in the rotating-beam channel at Admiralty Research Laboratories.

Thirteen small Ott-type current meters having propeller diameters of 50 mm, nominal hydraulic pitch 25 mm and electric contact for each revolution, were mounted on a special frame as shown in Fig. 5.5. The meters were rated simultaneously in preference to single or four-meter batch rating used by Ott.

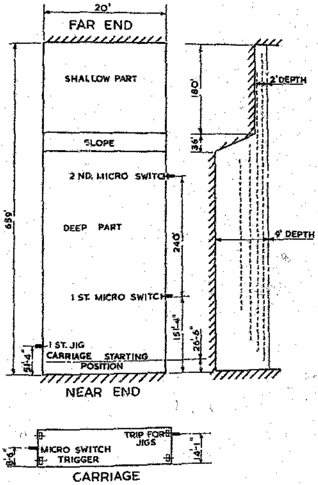

FIG. 5-6 NO. 2 TOWING TANK N.P.L.

No. 2 towing tank at N.P.L., in which the tangential ratings were performed, is shown in Figs. 5.6 and 5.7; the latter figure illustrates the position of the supporting frame in the tank. The towing carriage was equipped with an electronic speed control of the closed-loop automatic type which ensured constancy of a set speed within close limits.(69) It was of very light and rigid construction and, as far as could be ascertained, did not vibrate in the speed range of the rating tests.

In the recording equipment a quartz crystal transistor frequency standard, accurate to 1 part in 10^6, was used as time standard. Post Office relays were employed in the autotimer to generate time signals which could be selected in the range 5 to 1000 seconds. Each propeller meter operated a sensitive relay which in turn drove an electromagnetic counter capable of operating at up to 25 counts per second. The counters could be reset electromagnetically to zero, while records of the time interval chosen and the number of the test were supplied by two counters on the autotimer panel which were duplicated on the main counter panel to facilitate photographic recording of readings.

In the first test series at N.P.L. records of the carriage speed were obtained for each [illegible] run from a chronometer started and stopped by [illegible]

No. 2 towing tank at N.P.L., in which the tangential ratings were performed, is shown in Figs. 5.6 and 5.7; the latter figure illustrates the position of the supporting frame in the tank. The towing carriage was equipped with an electronic speed control of the closed-loop automatic type which ensured constancy of a set speed within close limits.[69] It was of very light and rigid construction and, as far as could be ascertained, did not vibrate in the speed range of the rating tests.

In the recording equipment a quartz crystal transistor frequency standard, accurate to 1 part in 10^6, was used as time standard. Post Office relays were employed in the autotimer to generate time signals which could be selected in the range 5 to 1000 seconds. Each propeller meter operated a sensitive relay which in turn drove an electromagnetic counter capable of operating at up to 25 counts per second. The counters could be reset electromagnetically to zero, while records of the time interval chosen and the number of the test were supplied by two counters on the autotimer panel which were duplicated on the main counter panel to facilitate photographic recording of readings.

In the first test series at N.P.L., records of the carriage speed were obtained for each calibration run from a chronometer started and stopped by micro-switches

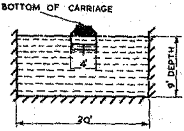

FRAME IN CROSS-SECTION OF TOWING TANK

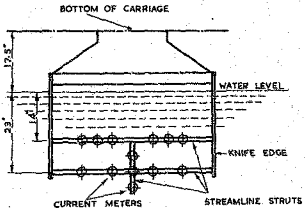

FIG. 5·7 POSITION OF SUPPORT FRAME IN TANK RELATIVE TO CARRIAGE, SURFACE AND WALLS.

at the beginning and end of a recording distance of 240 feet. In the second test series, the recording distance was varied, beginning and end signals being transmitted from rail jigs 20 feet apart; the chronometer was replaced by the crystal transistor frequency standard which supplied the time signals for a preselected number of jigs on the autotimer.

In the circular rating tests at A.R.L., the same meter supporting frame was used and was bolted to the rotating beam; its centre line was located at a radius of 49.895 ft. (Fig. 5.7), allowing for submergence identical to that for the N.P.L. tests. The motor driving the rotating beam was energized from a Ward-Leonard motor-generator set, with speed control by generato. excitation. Beam speed was controlled automatically by a closed loop servo system which received its signal from an accurate tachometer driven by the rotation-beam motor. Towing speeds for the 50-feet-radius towing path were read in ft/sec from a cintel counter by means of a suitably dimensioned gear wheel which rotated between the pole shoes of a magnet. Speed corrections were made in accordance with meter positions relative to the centre of rotation [(69), (84)]

Water temperatures throughout the tests were constant at 15.5°C for the first and 17°C for the second

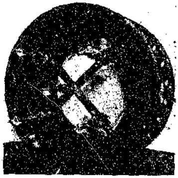

FIG. 5·8 TESTS ON 20 INCH LINE

test series, respectively, while waiting periods between test runs varied from 5 to 15 minutes. The second rating series was carried out after the meters had been used on a hydro-electric field test series. Results are discussed presently.

4.1.2 Application on 20-inch calibration line

Five of the calibrated meters were selected to be installed in the 20-inch calibration line in the laboratory at N.E.L.

The test arrangement consisted of a flow line supplied from a constant head tank, control valve with diverter and electronic timer, and a collecting tank suspended on a weighbridge and is described in detail in reference [85]. On this rig, discharge determination by means of weighing gave results to within ± 0.2 per cent.

The five meters were mounted on a supporting cross in interference-free positions as shown in Fig. 5.8. The streamlined sections of the supporting cross were identical to those used on the calibration supporting frame. Meter positions were chosen in accordance with the log-linear rule with a fifth meter on the pipe centre line to help define the velocity profile.

The recording gear was the same as that used in the calibration experiments, and the speed range was approximately $0.6 \text{ m/s} \leq V \leq 2.8 \text{ m/s}$.

For each current meter reading there were as many as three weighing tank measurements of which the variation was for the greater part to the order of 1 in 1000. Results are discussed later.

4.1.3 Field application at a hydro-electric installation

As apparatus and methods were primarily developed for field application, it was decided to include in the research programme an experimental series of comparative flow measurements at a hydro-electric power station.

In these tests, pitot tube, salt-dilution, salt-velocity and current meter methods were applied simultaneously; the last mentioned was used as the test reference.[(79), (80)]

The thirteen small Ott current meters were mounted on a specially designed cross constructed from the same streamlined sections used for the supporting frame in the calibration experiments. The supporting cross, with meters, was installed in one of the 40-inch-diameter hydro-electric penstocks near the power house.[(67)] The meters were mounted in interference-free positions

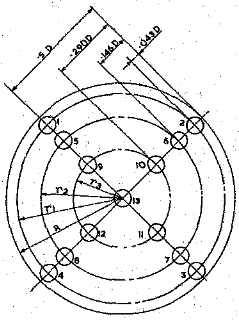

VIEW LOOKING UPSTREAM

POSITION No	METER No
1	9154
2	9160
3	9162
4	9166
5	9155
6	9156
7	9163

POSITION No	METER No
8	9164
9	9157
10	9159
11	9161
12	9165
13	9167

R	r_1	r_2	r_3
0·4980	0·4552	0·3526	0·2092

FIG. 5·9 POSITIONS OF THE 13 MIDGET CURRENT METERS IN THE PIPELINE, STATION 1.

in accordance with the requirements of the German code and the log-linear law. See Fig. 5.9.

The use of small current meters was dictated by the fact that the pipe diameter, one metre, was too small to accommodate an adequate number of standard-sized meters in interference-free positions. Both pipe diameter and meter size were therefore less than the permissible minimum specified by the Power Test Code.[16]

The internal pipe diameter was measured accurately by means of a specially designed rotating scale; the meters were wired up and the cables taken through a standard plug in the pipe wall before being cemented into position with liquid araldite.

A second current meter station was equipped with four standard-size Ott meters arranged on four radii at a distance of 0.112 D from the pipe wall boundary as specified by the log-linear law. In the 20-inch calibration line tests, the small Ott meters at these log-linear positions gave reasonable results and so it was decided to establish this second experimental station in order to compare the performance of the standard-sized meters at this nearwall position with that of the small meters at the first station.

4.2 Discussion of results in the light of the factor analysis

In these experiments, the manufacturer's original ratings and those determined from the second re-calibration agreed with the initial ratings for most of the meters to within ± 0.5 per cent, all but two being within ± 1 per cent.

The conditions in the rating tank, the experimental procedure, and the recording method remained unchanged for the two tangential rating experiments. Since, by comparison with the Ott characteristics, higher towing velocities were required in the first rating tests to produce the same number of meter counts, it seems justifiable to attribute the differences to ageing of the current meters. The discrepancy limit of 1 per cent between the two tangential ratings, two months apart, points to a possible increase in internal meter friction, conceivably due to the fact that in the field test the meters remained submerged in contaminated water for several days between the two ratings. Subsequent inspection revealed that the meter bearings were soiled.

The systematic error of the meter calibration was approximately ± 0.1 per cent, the random standard deviation approximately ± 0.25 per cent, and the overall standard deviation approximately ± 0.27 per cent. The

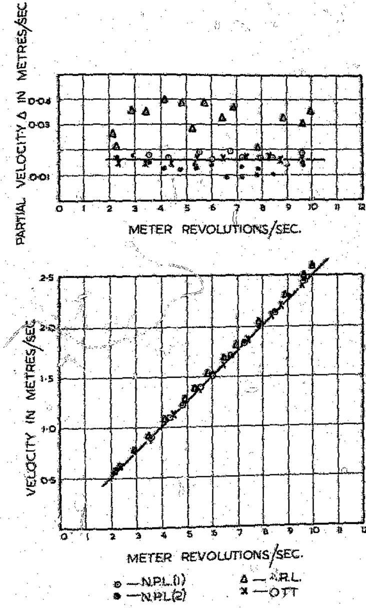

FIG. 5·10 CALIBRATION RESULTS FOR METER U.9166.

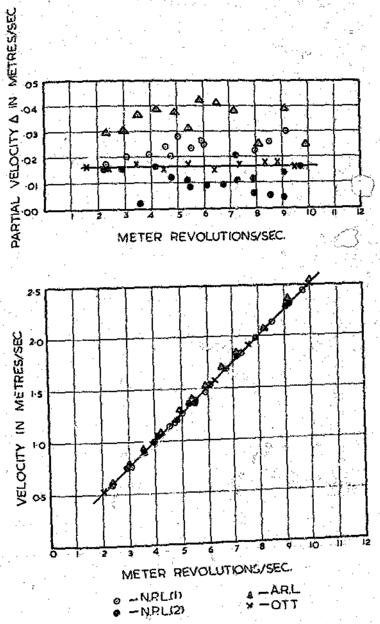

FIG. 5·11 CALIBRATION RESULTS FOR METER T 9165 experimental results fell within the 95 per cent confidence limit band. (Figs. 5.10 and 5.11).

Waiting periods varied between 5 and 15 minutes for the two ratings and the depth of submergence was held constant. The lack of any discernible influence of these factors on the rating results could probably be attributed to the size of the supporting frame relative to tank dimensions.

Grouping the current meters into rings of four limits the deviations between the two towing-tank ratings to approximately ± 0.6 per cent, for the group results, as shown in Fig. 5.12; this represents the two extreme groupings. A summary of meter grouping results for N.P.L. and Ott ratings is shown in Fig. 5.13. It is evident that, in still water ratings, any changes in meter characteristics would be identifiable.

The results for the circular rating tests gave systematic differences of the order of +2 per cent when compared with the first towing-tank results. This was probably caused by swirl induced in the direction of motion by the passage of the supporting frame and meters through the water. The recorded velocity would therefore be less than the set beam speed in still water. Typical experimental rating characteristics are shown

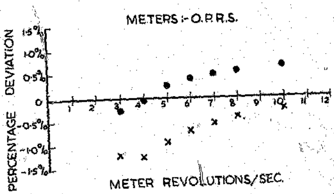

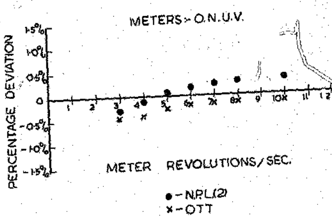

FIG. 5·12 DEVIATION OF ARITHMETIC MEAN OF THE RESULTS OF TWO GROUPS OF FOUR METERS FROM THE FIRST TOWING TANK RATING

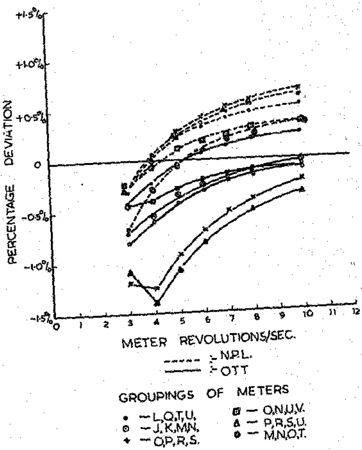

FIG.5·13 SUMMARY RESULT OF METER GROUPING in Figs. 5.11 and 5.14. In most of the meters, there seems to be a slight tendency towards a decrease in deviations with increasing towing speed. If this is true it is probable that the increased swirl effect is offset by a reduction in internal and hydraulic meter friction which, in turn, could be attributable to vibration of the rotating beam at higher speeds. On the other hand, a certain degree of turbulence prevails at the higher beam speeds and consequently the swirl effect could also be counteracted by an over-registration due to turbulence; the result would be a reduction of error. The results in the rotating beam channel seem to confirm the oft-voiced critisism of circular path rating of current meters.(65)

Four meters in the 20-inch diameter calibration line at N.E.L. gave six values of discharge to within a maximum error of about +0.2 per cent, for flows between 14 and 19.5 cusecs, while at approximately 10.5 cusecs one value differed by as much as -0.4 per cent from the gravimetric discharge measurements. In this particular application, therefore, still-water ratings seem in general to be adequate and accurate. Further analysis of this statement is, however, necessary. (See Appendix IV Table IV.1).

Upon examination of the original experimental work

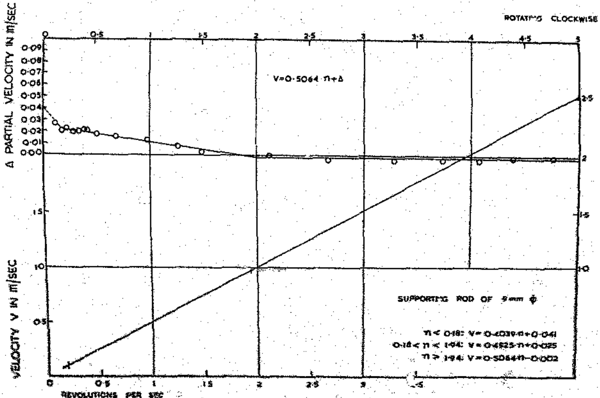

FIG. 5·14 EXAMPLE OF RATING CERTIFICATE FOR OTT-SMALL TYPE CURRENT METER and calculations, the author noticed that below a meter speed of 6 revs/sec, two test runs showed negative discrepancies which increased with decreasing flow rate. These results were originally not tabulated because they fell outside the speed range for the hydro-electric field test which was $6 \leq n \leq 10$. At flow rates of 6.7 and 4.0 cusecs, these discrepancies were approximately -2.0 and -3.2 per cent respectively, for corresponding n-values of $2 \leq n \leq 4$. The meter characteristics were valid down to $n \geq 2$.

Plotting of the individual meter readings disclosed a particular form of velocity profile at the gauging section below a flow of approximately 7 cusecs. Between this and approximately 10.5 cusecs there was a transition to an altered form of velocity distribution, while flow rates above 10.5 cusecs gave a similar but more developed profile form.

Thus, below a flow rate of approximately 10.5 cusecs, errors are negative and increase with decreasing flow rate to a maximum of -3.2 per cent, while small random positive errors of +0.2 per cent maximum value result for flow rates above 10.5 cusecs.

According to the factor analysis in the foregoing section, over-registration and hence over-estimation of flow rate and negative errors are caused by the supporting frame; velocity interference effects, on the other hand, would give rise to under-registration and therefore positive discrepancies. The effect of rating in still water is admittedly unknown, but the other factors have been known to have no appreciable influence in the lower flow ranges. It therefore appears that at low velocities proximity effects are masked by those due to frame and velocity gradient and yield a negative error. This was indeed substantiated by Ott (66) who reported that interference effects at lower velocities were insignificant. It is also in agreement with the author's hypothesis concerning the structure of proximity interference advanced in sub-section 3.23.

At the higher velocities, however, a certain degree of turbulence together with increased velocity gradient, and frame effects - all of which cause negative errors - are masked by the positive error due to proximity interference effects, and therefore a smaller positive error would result.

This explanation agrees with Ott's findings (66) that meters near a wall showed errors of -2.1 per cent at a velocity of 2.5 m/s, and that this causes a positive error of approximately the same magnitude as the negative error due to the frame and velocity gradient effects at

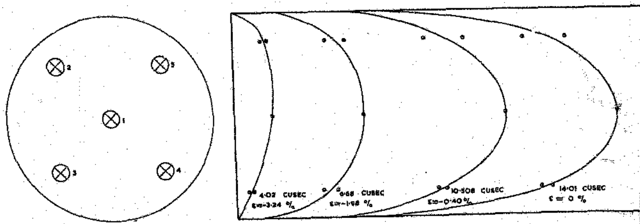

FIG.5·1: VELOCITY PROFILES FOR DIFFERENT DISCHARGES IN THE 20-INCH CALIBRATION LINE

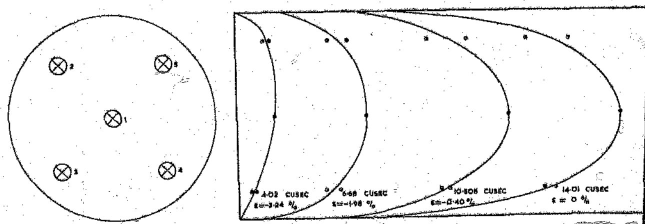

FIG.5·15 VELOCITY PROFILES FOR DIFFERENT DISCHARGES IN THE 20-INCH CALIBRATION LINE the lower velocities.

The meters seem to be sensitive to velocity profile effects. Fig. 5.15 shows approximate profiles indicating the steep gradients at some flow rates. The plot of individual meter velocities also revealed that, up to and slightly beyond 6.7 cusecs discharge, velocities, in decreasing order of magnitude, were to be found at meter positions 1-2-3-5-4 while at 10.5 cusecs and above, the velocity order changed to 1-2-3-4-5, i.e. it became cyclic anti-clockwise. Consequently meters 4 and 5 were subjected not only to steep velocity gradients but also to a change-over in profile-form at some flow rate between 6.7 and 10.5 cusecs. The corresponding errors at these two flow rates are -1.98 and -0.4 per cent.

As discussed earlier, Ott (66) found that proximity interference effects were negligible in the velocity range 0.1 to 1 m/s. Since the velocity at the above critical discharge is approximately ~~in~~ this range, the contribution, by proximity effects, to an error difference of approximately -2.0 and -0.4 per cent would be small. Thus it seems possible that velocity gradient and changes in it were mainly responsible for the large error difference.

Clearly, in this particular experiment, proximity interference and velocity gradient effects - together with smaller contributions due to turbulence and supporting-frame effects - all combined to yield errors varying between +0.22 and approximately -3.2 per cent in flow rate measurements over a range of 4 to 19.5 cusecs.

It should be stressed here that effects due to proximity interference and supporting frame also tend to alter the velocity profile which was shown to have such a marked influence on meter performance. This, together with the difference in velocity distribution under conditions of towing and flowing is the crux of the problem.

The above analysis questions the validity of accepting the results of the 20-inch line tests as a verification of the accuracies claimed in the field tests at Kinlochleven, where the effects of the factors involved were unknown.

In the field tests at Kinlochleven, the current meters gave the most consistent results. The standard deviations of the results - computed by log-linear method - from the readings of eight small meters at Station 1 - were the smallest recorded; the deviation from the flow rates determined graphically using all thirteen meters was less than 0.5 per cent.

Results obtained from the second current meter station, equipped with four standard-sized meters, were within 1 per cent of the reference at the lower flow rates but differed by as much as 2 per cent at the higher rates of flow. In these experiments, however, only comparative and not absolute accuracies were possible; the current meter results were used as reference. The results at the second station show that the discrepancies increase at higher flow rates, probably due to the proximity interference and velocity gradient effects on meters of larger diameter.

The meters were subjected to line pressures of approximately 370 lb/in.^{2} and 390 lb/in.^{2} and were submerged for more than 72 hours.

In recent experiments carried out by N.E.L. and Swiss (86) teams at Fätschbach in Switzerland, thirteen identical miniature Ott current meters gave results having standard deviations of less than $\pm$ 0.2 per cent around the means of 114 results arranged in 21 groups. A second station which was equipped with five normal-sized meters (one at the pipe centre line) gave results at the higher flow rates which were within +2 per cent of the reference, while the lower discharge rates yielded results affecting the operation of current meters dictate the accuracies of measurements. This analysis illustrates the marked influence of velocity gradient, proximity interference and frame effects on a single ring of meters near a solid boundary when measurements are interpreted in terms of still-water ratings.

When thirteen current meters are arranged in three concentric rings, the factors discussed come into play and although, as shown, accuracies of ± 1 per cent can be achieved under certain conditions, such accuracy cannot be guaranteed.

5. CONCLUSIONS

The foregoing factor analysis has accentuated the importance of the difference in flow structure between conditions of towing and flowing. The author is of the opinion that future research should be aimed at developing a method by which current meters can be rated in flowing instead of still water, the individual meters being arranged in the exact positions in which they are to be used.

It is suggested that fully developed flow profiles can be established experimentally in a pipe or a flume. As a separate study, the turbulent structure and oblique flow components can then be determined for various flow rates, followed by total pressure traverses with wall static tappings to determine the corresponding velocity profiles. Total pressure and static hole errors as described in the previous chapters must not be overlooked.

The next step would be the determination of flow rates directly by means of accurate volumetric measurements in a calibrated tank of suitable capacity, from which the velocity profiles as determined above could be corrected. Applying the log-linear law, these corrections would simply entail adjusting each individual velocity determination by p per cent where

$$p = (\bar{V}_t - \bar{V}_m)100,$$

in which $\bar{V}_t$ = average velocities as determined from the calibration tank, and

$\bar{V}_m$ = average velocities as determined from the total pressure traverses for each velocity profile.

At this stage, accurate velocity profiles at the measuring section would have been established for corresponding rates of flow.

The current meters on a supporting frame, or individual meters, can then be placed in position. For each flow rate a particular meter would be subjected to a flow velocity determined from the corresponding velocity profile and meter position in the gauging cross-section, whereupon meter speeds could be recorded for different velocities of flow at the actual meter positions. In order to assess the effect of distortion of the velocity profile due to the presence of the supporting frame, a corrected velocity profile could be determined at a section, in the plane of the meter propellers, with meters and supporting frame in position. These velocities could then be used, as outlined above, to calibrate the meters at various flow rates in flowing water. Initial experiments, based on the above suggestions, would probably precipitate further development and refinement.

If, as discussed in the previous chapters, future research can render more accurate the measurement of total and static pressure, this suggested calibration method would certainly be possible. It is also evident that the effects due to factors such as turbulence, supporting frame, oblique flow components, velocity gradients, meter proximity interference, and towing would be reflected directly in a meter's calibration characteristics. It is also possible that the same current meter might have different rating characteristics, depending on its position in a pipe or flume cross-section or the degree and structure of turbulence and angularity of flow. The influences of the other factors can also be studied in flowing water in accordance with this suggested method.

The basic principles and factors affecting the operation and performance of propeller-type current meters have been analysed and suggestions have been made for the possible development of more accurate and refined techniques for meter calibration and application. The author trusts that these will be of some value to research workers and would-be users of current meters.

C H A P T E R VI

THE MEASUREMENT OF DISCHARGE - THE VENTURI METER

1. INTRODUCTION

In many fields of engineering measurements of flow rate are demanded to accuracies far higher than those laid down by the various National Standards. One of the earliest instruments for measuring discharge is the venturi meter to which this chapter is devoted.

In Chapter I, it was indicated that little or no systematic analysis had been made of the theoretical and experimental factors affecting the operation of venturi meters and that a review of existing knowledge on flow through venturi meters had revealed many controversial points which demanded clarification and solution.

In 1797, the principle underlying the conversion of energy in a convergent-divergent tube was postulated by Venturi [87] who had only academic interest in the matter. Clemens Herschel [88] then introduced an instrument for measuring the flow of water. A meter, almost identical to the modern venturi meter, was originally developed by Bourdon for measuring the flow of air in mines.[87] Herschel, however, was probably the first to determine the flow of water by measuring the ~~pressure~~ difference between main and throat pressures.

The original meter theory was based on Bernoulli's equation as applied to simple one-dimensional flow. For incompressible fluids this yields the relationship :

$$Q = C_d \frac{A_2}{\sqrt{(1 - \frac{A_2}{A_1})}} \sqrt{\frac{2}{\rho} . \Delta_p} \quad \ldots\ldots(6.1)$$

where

Q = quantity discharged;

C_d = coefficient of discharge;

A_1 = cross-sectional area at inlet to the meter;

A_2 = cross-sectional area at venturi throat;

Δ_p = measured pressure differential, and

ρ = mass density of fluid.

Departure from one-dimensional flow conditions assumed, effect of shape of velocity profiles, friction and boundary-layer effects, and the influence of pressure gradients all serve to make C_d a complex function.

One of the first research workers to study factors affecting C_d-values was Gibson,[89] who in 1915 attempted to predict values for the discharge coefficient. He demonstrated that C_d depended upon, among other factors, the velocity profile at the gauging sections and on the friction losses through the meter.

Pardoe [90] investigated the possibility of predicting values for C_d in 1919. He calculated the total losses between the entrance and throat sections, but neglected the effect of velocity distribution which was shown by Gibson to be of paramount importance.

Factors other than surface roughness were set out very clearly in Ref. 91 where test data from different countries were used for deriving empirical values for the discharge coefficient, without evaluating the actual effect of the different factors involved.

A comprehensive analytical approach to this problem was attempted by Engel and Davies [92] in 1938, and again by Engel in 1953. [93] Engel suggested correction factors to account for non-uniformity of velocity distribution outside the boundary-layer at the measuring sections. He dealt with an impact correction factor to account for the inward bending of streamlines in the converging portion of the meter; he briefly mentioned boundary-layer growth but ignored friction losses in the meter as well as adverse pressure gradients. He derived no expression for C_d and his mathematical treatment of the so-called 'impact pressure' does not seem to be correct.

In a valuable contribution in 1954, Hutton [87] suggested a theoretical relationship for C_d in which he considered velocity distribution correction factors and losses through the venturi. Inward bending of streamlines, curvature of streamlines, and boundary-layer growth were not considered. He pointed out the possible effects of these factors on the discharge coefficient, inviting further analysis and research.

Rivas and Shapiro [94] developed a theoretical relationship for the discharge coefficient of rounded-entrance meters. Their theory is based on an effective friction length at entrance, boundary-layer growth, and potential flow in the core outside the boundary-layer. Although good agreement between experimental and theoretical results was obtained, their method deals with a particular type of instrument and pressure tapping, and the authors neglected some of the factors mentioned above.

Recently, Hall [1] suggested a solution which has evoked great interest. He ignored all factors influencing C_d and merely considered theoretically various features of flow in a throat boundary-layer. He compared his theoretical results with those obtained in experiments on a 4-inch venturi meter with which the author was associated at N.E.L. The agreement was remarkably good over the laminar region. Some authorities argued that the solution could hardly be as simple as it appeared, while others welcomed Hall's method as a progressive approach.

The author is of the opinion that the mere accumulation of masses of experimental data, without basic factor analysis and theoretical treatment, cannot lead to improved accuracies in venturi meter measurements.

2. THE VENTURI METER PROBLEM

The above, together with the analysis in Chapter I, clearly outlines the difficulties associated with flow through contractions. This problem was recently aptly formulated by Engel who, to quote him once more, stated that : 'The main task in the near future would be to advance certain hypothesis and to confirm or refute them, systematically narrowing down the wide scope of contradictory arguments, and thus, establishing a better insight into the mechanism of flow through contractions.'

The desire to obviate meter calibration - an elusive and challenging goal - prerequisites a comprehensive theoretical analysis of venturi flow, since this could lead to relationships for predicting C_d-values within specified limits of accuracy.

A possible theoretical expression for C_d which incorporates Hutton's and Hall's theories and in addition allows for effects of turbulence and wall static pressure errors, could be of value in attempting to assess the hitherto unknown influences of the various factors affecting flow through venturi meters.

In this chapter, the author has analysed each of the controversial factors and developed a theoretical relationship which gave C_d-values in close agreement with those determined experimentally. Extension of the above theory yielded a second expression for C_d which is recommended for future research.

3. ANALYSIS OF THE FACTORS AFFECTING VENTURI METER OPERATION

The following factors are analysed :

3.1 Upstream pipe roughness.

3.2 Upstream velocity profile.

3.3 The length of straight upstream pipe.

3.4 The throat boundary-layer.

3.5 The impact pressure.

3.6 Losses over the venturi meter.

3.7 The static pressure error.

3.8 Turbulence.

3.9 Rounding of upstream and throat entrances.

3.10 Upstream and throat tapping positions and throat length.

3.11 Internal meter roughness.

3.12 Rounding of the inside edges of the pressure tapping holes.

3.13 Angles of contraction and diffusion.

[illegible] Method of pressure tapping.

[illegible] Other factor influences.

[illegible] Upstream pipe roughness effects

It is known that C_d increases with increasing upstream pipe roughness. Schlag[21] experimented on 'smooth' and 'rough' pipes having f-values of 0.015 and 0.025 respectively and found that C_d increased approximately 0.5 per cent over the test range at high Reynolds numbers.

The original roughness value or coefficient of friction would however change with time due to the formation of internal deposits on the pipe wall. Deale[17] reported that a mossy growth inside a 36-inch diameter upstream pipe gave a discharge coefficient 1 per cent below the value obtained after the growth was removed. He also found that internal cleaning, cleaning and painting, and lining with smooth concrete, caused variations in the values of C_d of up to +6 per cent for a 36-inch x 16-inch venturi meter.

It is important to note that upstream pipe roughness, which tends to vary with use and age, also affects other factors listed above. Changes in roughness affect the upstream velocity profile, which in turn influence C_d. If roughness variation is caused by internal grit deposits, the pipe cross-sectional area changes accordingly, thereby affecting C_d-values. Hall [(1)] submits that roughness affects the throat boundary-layer thickness which, according to his hypothesis, controls the value of C_d.

According to Engel [(3)] the form of the velocity profile at entrance, and therefore the upstream pipe roughness, also affects the impact pressure factor. He further pointed out that in order to eliminate or minimize effects due to conditions in the approach pipe, a 'pointed' velocity profile having a high velocity at the conduit axis must be aimed at.

Hutton [(87)] showed that changes in C_d, due to variation of upstream pipe roughness, could be eliminated by keeping m, the area ratio, less than 0.3.

It seems necessary to devise a method whereby 'roughness' can be precisely defined and controlled -

a requirement which is at present not satisfied.

3.2 Upstream and throat velocity profile effects

When Bernoulli's Theorem is applied to a venturi meter, the velocity terms refer to the mean velocities at the gauging sections and uniform distribution of velocity is assumed. Correction should be made for non-uniformity in velocity distribution outside the boundary-layer by introducing kinetic energy coefficients in the Bernoulli equation, when calculating experimentally determined C_d-values.

Engel (3) showed that it was reasonable to assume a gradual increase in discharge coefficient towards unity as Reynolds numbers increased to 10^7 or higher. Although not verified as yet, this is probably due to velocity profile changes. Engel also suggested that to minimize the effect of this factor upstream velocity profiles for conditions of calibration and application should be approximately identical. The difficulties associated with this requirement in practice are self-evident.

Schlag (21) reported experiments with high diameter-ratio meters which showed that the 'hump' in the rating curve disappeared when rough upstream pipes were used. This factor is referred to here since the author is of the opinion that the 'hump' is caused in part by a velocity profile effect which, in turn, is influenced by the upstream pipe roughness.

Engel [(3)] suggested the desirability of a 'pointed' upstream velocity profile in order to minimize the effects of changes in upstream pipe roughness. On the other hand, this would demand an increase in the kinetic energy correction coefficient for the velocity profile at entrance. If such a 'pointed' profile should be distorted by upstream pipe fittings, the correction coefficient would be subject to an unknown and variable error.

This velocity profile factor is also coupled to other factor effects. It is directly or indirectly related to upstream pipe roughness, Reynolds number, approach pipe length, upstream pipe fittings, impact pressure and throat boundary-layer; the effect can be studied theoretically and evaluated in the form of a kinetic energy correction coefficient, provided that the upstream velocity profile is known. This is dealt with presently.

3.3 The effect of the length of straight upstream pipe

It is essential to ensure a fully developed velocity profile at entrance to the venturi and accordingly the effect of this factor can be eliminated by providing a sufficient length of straight upstream approach pipe. At N.E.L. lengths of from 42 D to 77 D - depending on the meter size and the type of test rig used [2], [95] - proved satisfactory.

3.4 The effect of the throat boundary-layer

In a recent paper, Hall [1] suggested that the value of a discharge coefficient was determined ~~mainly~~ by the throat boundary-layer thickness. The displacement thickness of the layer was considered analogous to a thin-walled uniform-bore tube, inserted into a venturi throat, thereby altering the throat cross-sectional area from A_2, to A_2'. He consequently defined the discharge coefficient simply as $C_d = \frac{A_2'}{A_2}$, which renders C_d dependent only on the throat boundary-layer.

His theory is based on a simple flow model. It is assumed that throat boundary-layer development is identical to that for a flat plate with zero longitudinal pressure gradient, and that all the factors influencing the flow through a venturi meter would automatically be embodied in the throat boundary-layer characteristics which, depending on the different factor effects, could be either laminar, turbulent, or both. He made several assumptions which seem rather liberal and unsubstantiated. The approach, however, was refreshing. Nevertheless, the degree of conformity between Hall's theoretical curves for laminar boundary-layer flow and a selected number of N.E.L. experimental values over a limited Reynolds number range, could hardly be considered as adequate verification of his assumptions.

Boundary-layer growth in a nozzle and throat is admittedly important, but no convincing explanation was submitted for neglecting the effects of the other factors involved. Hall's theory implies, for example, that losses over the meter, as well as the effect of factors such as velocity profile, impact pressure, roughness effects, turbulence and static pressure errors - to mention only a few - are all incorporated in the boundary-layer characteristics. This is clearly unacceptable.

On the other hand, it should be pointed out that this theory enabled Hall to explain some of the irregularities shown by C_d vs R_e calibration curves which had been ignored by most investigators in the past. Hutton's theory could, however, also be adopted to provide acceptable hypothesis as will be illustrated later.

In a stimulating discussion of reference 1, many leading authorities provided useful data on this boundary-layer concept, but little agreement was reached concerning its mechanism and effects.

Three important questions seem to emerge from the above study, namely :

3.4.1 Is the throat boundary-layer the only crucial factor?

3.4.2 Can the throat boundary-layer thickness be treated, theoretically, as analogous to that developed on a semi-infinite flat plate with zero longitudinal pressure gradient?

3.4.3 Can the throat displacement thickness be considered as analogous to the introduction of a uniform-bore tube in the throat, representing the 'displaced' boundary wall of the throat?

The above questions can be analysed thus :

The author is of the opinion that the first question should be answered in the negative : It would be safer and decidedly more logical to consider boundary-layer effects in association with the listed factor effects.

Controversy with regard to the second question exists inasmuch as it was pointed out, in the first place, by several experts,[1] that a length much greater than a throat diameter would be required to ensure a fully developed laminar or turbulent boundary-layer in a venturi throat. (Hall used the relationship $\ell = d$ in his theoretical calculations). Secondly, the unknown pressure gradient in the throat affects boundary-layer growth and probably excludes the analogy of a semi-infinite flat plate with zero longitudinal pressure gradient. It can also be argued that the analogy is not applicable because of the difference between flow conditions associated with boundary-layer growth on a flat plate and that in a circular duct with totally confined flow.

Discussing Hall's paper, Hutton pointed out that it might be acceptable to write $\ell = d$ for a nozzle-type venturi meter, but certainly not for a conical-type meter such as the one tested at N.E.L. He suggested that a value of $\ell = 1.3$ d would probably be more justifiable according to his findings described in reference 87.

In the above discussion, Engel referred to work done by Hahnemann and Ehret (96) on boundary-layer growth in a narrow rectangular channel fitted with an entrance nozzle. This investigation showed that relatively long distances were required to ensure fully developed laminar or turbulent boundary-layers. The author studied these experiments but cannot agree with Engel that this narrow channel model showed greater similarity to flow conditions in a closed conduit than that over a semi-infinite flat plate. The mere presence of a so-called 'second rigid boundary' in the absence of a pressure gradient in fully confined flow does not seem to establish this model as a more acceptable alternative.

In the same discussion, Ryley and Barrow reported that they had applied the boundary-layer principle but recommended the use of the momentum integral equation instead of the semi-infinite flat plate analogy. This would probably be more correct.

The author is of the opinion that the flat plate analogy would be applicable if sufficient length for boundary-layer development is allowed in the calculation of the maximum displacement thickness in the throat. The effect of ignoring the pressure gradient in the analogy is not known, but it certainly affects boundary-layer stability and hence the displacement thickness in both laminar and turbulent conditions of flow. At an established condition, however, a small change in displacement thickness caused by a pressure gradient in a venturi throat should have little effect on C_d. If boundary-layer control could ensure a turbulent throat boundary-layer over an entire flow range, as has been suggested,(1) the semi-infinite flat plate analogy would be approximately applicable. Question three regards the principle of treating the displacement thickness as being analogous to a thin-walled tube in a venturi throat which, in effect, reduces the actual throat diameter, and hence the area ratio m. This approach was suggested by the author at N.E.L. in 1957; the idea was never applied however, because of lack of experimental data at the time on throat boundary-layers and velocity profiles.

Under normal conditions of flow in a pipe, this analogy would certainly apply since, according to the Prandtl hypothesis, viscous influences are confined to developing wall boundary-layers while inviscid irrotational flow occurs in an outside fluid core which moves forward at constant velocity. On the strength of its concept and definition the displacement thickness of a boundary-layer can therefore be considered as an internal concentric thin-walled tube which, in effect, decreases the theoretical effective cross-sectional area through which flow takes place. In order to evaluate the displacement thickness, it is essential to know whether the flow in a boundary-layer is laminar or turbulent.

Assuming a laminar boundary-layer to exist at entrance to a venturi meter, this layer is subjected to